Article

Published in *ChemPhysChem*, 11, 1, 195-210 (2010) **DOI: 10.1002/cphc.200900509**

Hydrogen radical addition to unsaturated hydrocarbons and reverse β-scission reactions: modeling of activation energies and pre-exponential factors

Maarten K. Sabbe,[a] Marie-Françoise Reyniers,*[a] Michel Waroquier,[b] and Guy B. Marin[a]

The group additivity method for Arrhenius parameters is applied to hydrogen addition to alkenes and alkynes and the reverse β-scission reactions, an important reaction family in thermal processes based on radical chemistry. A consistent set of group additive values for 33 groups is derived to calculate the activation energy and pre-exponential factor for a broad range of H-addition reactions. The group additive values are determined from CBS-QB3 ab initio calculated rate coefficients. A mean factor of deviation between the CBS-QB3 and the experimental rate coefficients for 7 reactions of only 2 in the range 300-1000 K is found. Tunneling coefficients for these reactions were found to be significant below 400 K and a correlation accounting for tunneling is presented. Application of the obtained group additive values to predict the kinetics for a set of 11 additions and β scissions yields rate coefficients within a factor 3.5 from the CBS-QB3 results except for 2 β scissions with severe steric effects. The mean factor of deviation with experimental rate coefficients is 2.0, showing that the group additive method with tunneling corrections can accurately predict the kinetics, at least as accurate as the most commonly used density functional methods. The constructed group additive model can hence be applied to predict the kinetics of hydrogen radical additions to a broad range of unsaturated compounds.

Introduction

The addition of hydrogen radicals to alkenes and its reverse β scission, are important elementary steps in radical processes such as polymerization, pyrolysis, steam cracking, partial oxidation and combustion.[1] Therefore, the reaction family of hydrogen addition/β scission forms an indispensable part of any radical reaction network.

A reliable reactor optimization requires an accurate kinetic model based on elementary reactions. For radical chemistry, on which many of the world largest scale chemical processes are based, the reactive nature of the radical intermediates results in huge reaction networks typically involving hundreds of species and thousands of elementary reactions.[2-4] Currently, most elementary reaction networks are automatically generated using advanced algorithms for the selection of the relevant reactions.[5-11] Sensitivity studies on these reaction networks point out that the main part of the uncertainty on the product yields stems from inaccurate knowledge of kinetic data.[12,13] Therefore, accurate kinetic data are essential to obtain reliable process simulations. Moreover, if rate-based network construction algorithms are applied,[14] accurate rate data are even more important as inaccuracies can result in the construction of an incomplete network that is not capable of grasping the underlying chemistry of the process.

A quantitative description of radical processes thus requires that rate parameters be known for all of the different reactions comprising the reaction network. However, it is very difficult to measure kinetic parameters for individual radical reactions experimentally as these reactions are frequently coupled. Therefore a variety of methods for rate prediction of radical reactions has been developed. These methods range from correlating the activation energy to the reaction enthalpy, such as Evans-Polanyi correlations and its variations,[15-17] to more sophisticated methods based on the structure of the transition state. Several of the latter methods are related to Benson group

[a] *Prof.dr. Marie-Françoise Reyniers*
Laboratorium voor Chemische Technologie, Ghent University
Krijgslaan 281 S5, B-9000 Gent, Belgium
Tel.: +32 9 264 9655
Fax: +32 9 264 5824
E-Mail: mariefrancoise.reyniers@ugent.be
[b] *Center for Molecular Modeling, Ghent University*
Proeftuinstraat 86, B-9000 Gent, Belgium

Supporting information for this article is available on the WWW under http://www.chemphyschem.org or from the author

additivity.[18,19] Among these are: 1. the structural group contribution method of Willems and Froment,[20,21] in which correction terms on the Arrhenius parameters of a reference reaction account for structural differences between the latter and the considered reaction; 2. methods that calculate the thermochemistry of the transition state, such as the method described by Sumathi et al.,[22-24] 3. the Reaction Class Transition State Theory developed by Truong et al.[25,26] and 4. the group additive (GA) method for activation energies as described by Saeys et al.[27,28] Experimental determination of all the kinetic and thermodynamic parameters required for these methods is not possible due to scarcity of experimental data. Moreover, experimental determination of rate constants often involves assuming a reaction scheme which can induce a rather large scatter on the resulting reported kinetic data for a given reaction. Quantum chemical calculations can be applied to any reaction type, and extracting quantitative values of rate coefficients does not rely on assuming a reaction scheme. Therefore, the use of quantum chemistry to calculate rate coefficients for gas phase radical reactions is particularly attractive and the more recently developed parameterization schemes for carbon centered radical additions and β scissions[29] and for hydrogen abstraction[22-26] are all based on first principles calculations to determine the model parameters.

Although hydrogen additions are less commonly studied than hydrogen abstractions or non-hydrogen radical addition, rate coefficients for this reaction family are included in many literature reviews on radical reaction rate coefficients. In general, these reviews report not only experimental data but also predicted and extrapolated data. Hydrogen additions to hydrocarbons are included in, among others, the reviews of Baulch et al.[30,31] and Tsang[32-35], which concentrate on combustion chemistry, and the review of Curran[36] that summarizes experimental work on the decomposition of C_1 to C_4 alkyl radicals through C−C and C−H β-scission reactions.

The hydrogen addition to ethene is widely studied both experimentally[37,38] and using ab initio methods. Regarding ab initio studies, there are the early level of theory studies of Jursic[39] and Nguyen et al.,[40] indicating troublesome transition state determination with DFT methods for this hydrogen reaction, and an underprediction of the addition barrier. Fischer and Radom also showed that DFT methods tend to underestimate the barriers for hydrogen additions.[41] In general, addition to the most substituted carbon atom is slower than addition to the lesser substituted atom,[41] based on enthalpic and entropic considerations as well as on the evaluation of the carbon atom with the highest spin density in the alkene triplet, which will be the preferred site for radical attack.[42] Clarke et al.[43] studied the contribution of several properties to the barrier for hydrogen addition, revealing the dominant effect on the reactivity of the ionic state formed by transferring electron density from the alkene to the hydrogen atom. Using variational transition state theory and master equation analysis Miller and Klippenstein[44,45] studied the hydrogen addition to ethene, ethyne and 1,3-butadiyne. They showed that for these reactions tunneling effects have a large contribution to the rate coefficient at lower temperatures but that the effect disappears at T > 1000 K, and that the largest difference between conventional and microcanonical variational transition-state theory is, even at 2500 K, limited to 19% for H + ethene, 28% for H + ethyne and 15% for H + 1,3-butadiyne. Both approaches yield results within 10% of each other at temperatures below 1000 K and the variational effect decreases with temperature. Based on a 2-dimensional master equation analysis, Miller and Klippenstein[44] showed that, at 298 K, the reaction H + ethene already reaches the high-pressure limit at atmospheric pressure, while the rate coefficient of the highly pressure-dependent addition to ethyne under these conditions is only about a factor of 2 below the high-pressure limit. The findings of Miller and Klippenstein[44,45] justify the approach used in this paper, in which conventional transition state theory is applied to determine the rates for a large set of reactions in a temperature range of 300-1300K. Villa et al.[46-48] also showed the importance of the inclusion of tunneling effects for the H addition to ethene in describing the trends in kinetic isotope effects using variational transition state theory. These authors report that the addition to the most deuterium-substituted carbon atom is kinetically favored over the less substituted carbon atom.

In contrast to other reaction families, such as hydrogen abstractions, simple rate prediction methods for hydrogen additions are scarce in literature. The curve crossing model of Clarke et al.[43] allows predicting the barrier, but requires the inclusion of ionic and covalent excited states and is, as such, less suited to be implemented in automated network generation software. Denisov[49-51] includes hydrogen addition reactions in a general prediction method for radical addition activation energies based on the intersecting parabola model. The method includes addition to various substrates, including butadiene, styrene, triple bonds, C=O bonds and acrylonitrile. However, due to its complexity this method too is less suited for implementation in automatic rate prediction software. Moreover, both methods are limited to predictions of the activation energy and do not allow prediction of the pre-exponential factor. To the best of our knowledge, no structure-reactivity correlation covering a wide range of hydrogen additions to hydrocarbons is available in literature.

This work aims at the determination of a consistent set of group additive values (Δ*GAV*°) for the prediction of activation energies and pre-exponential factors of hydrogen additions to a broad range of hydrocarbons and the reverse C−H β scissions, in line with the recently reported group additive model for carbon-centered radical addition.[29] The computational approach involves conventional transition state theory based on high-level CBS-QB3 ab initio calculations,[52] which has already shown its accuracy for similar radical reactions in previous work.[27-29,53] In this paper, first the computational method is validated for hydrogen additions by comparing the CBS-QB3 rate coefficients with computational experimental data available in literature. Next, rate coefficients are calculated for 34 reactions, from which 33 group additive values are derived, and a model to correct for tunneling effects is proposed for rate predictions at temperatures below 1000K. Finally, the obtained group additive model is validated by comparing group additive predicted rate coefficients with ab initio calculated values and with experimental rate coefficients. The temperature range covered is 300-1300 K, which encompasses most chemical applications except combustion.

Computational methods

Transition state geometry

Rate coefficients are calculated according to the methodology described by Saeys et al.,[54] based on the CBS-QB3 method of Montgomery et al.[52]. It is well known that DFT methods, and in particularly the B3LYP functional[40,41] which is used for the geometry optimization in the CBS-QB3 compound method, pose difficulties to determine accurate transition state geometries for hydrogen addition reactions. Therefore, the transition state geometry is determined as described previously by Saeys[54]. First, the transition state is optimized at the MPW1K/6-31G(d) level using standard transition state search algorithms provided by Gaussian 03.[55] From this geometry the C−H_{MPW1K} bond length is extracted and is scaled using the correlation proposed by Saeys et al.,[54] to bring the MPW1K/6-31G(d) transition state geometries in accordance with IRCMax(CBS-QB3//B3LYP/6-311G(d,p)) geometries:[56]

$$C–H_{IRCMax} = 0.4904C–H_{MPW1K} + 94.07pm \qquad (1)$$

Finally, the transition state is reoptimized constraining the length of the forming C−H bond at the C–H_{IRCMax} bond length determined using equation (1). The reoptimization is performed using the B3LYP/6-311G(d,p) method used for the geometry optimization in the CBS-QB3 calculation. The obtained geometry is then applied for the calculation of the reaction barrier and the partition functions.

Rate coefficients

Rate coefficients are calculated using conventional transition state theory (TST) in the high pressure limit:[57]

$$k_\infty(T) = \kappa(T)\frac{k_B T}{h}\frac{n_{\mathrm{opt},\ddagger} q_\ddagger}{n_{\mathrm{opt},A} q_A n_{\mathrm{opt},B} q_B} e^{-\frac{\Delta E(0\ \mathrm{K})}{RT}} \qquad (2)$$

In equation (2) q represents the molecular partition function per unit volume, $\Delta E(0\ \mathrm{K})$ the electronic zero point corrected reaction barrier and $\kappa(T)$ the transmission coefficient accounting for quantum mechanical effects. The term n_{opt} in equation (2) corrects for the number of optically active isomers as the partition functions q pertain to a single enantiomer. The activation barrier at 0 K is determined with the CBS-QB3 complete basis set method of Montgomery et al.[52] All ab initio calculations have been performed using the *Gaussian 03* computational package.[55] Quantum tunneling coefficients, $\kappa(T)$, are calculated using the Eckart tunneling scheme,[58] as this tunneling method has already proven its reliability for radical reactions.[59-61]

Partition functions q are calculated using statistical thermodynamics based on the CBS-QB3 built-in B3LYP/6-311G(d,p) frequency calculation using a default scaling factor of 0.99. The partition functions are evaluated using the rigid rotor and harmonic oscillator (HO) approximation assuming separability of translational, external rotational, rovibrational and electronic contributions. Contributions of internal rotation to the rate coefficient are assumed to cancel out in the approximation that the internal rotations have a similar contribution in reactant and transition state. This holds for hydrogen additions since the addition of a hydrogen atom does not introduce a new internal rotor in the transition state; there is no internal rotation present around the forming C-H bond and due to the early transition state for addition reactions no rotation around the breaking π bond is possible yet. Only for β scission the HO approximation might influence the rate coefficients as the rotation about the forming π bond is more hindered in the transition state than in the reactant radical. The deviation introduced by the harmonic oscillator description of this rotation in the reactant radical is limited to, in the case of free rotation such as e.g. a methylene –CH_2 rotor, about a factor of 2 at 298 K and a factor of 3 at higher temperatures.

Arrhenius parameters were fitted to the ab initio calculated rate coefficient, i.e. without inclusion of the tunneling coefficient κ, using an Arrhenius fit with k sampled at intervals of 50 K between T-100 and T+100 K, with T the temperature of interest. The calculation of the partition functions, the tunneling corrections, the rate coefficients and the Arrhenius parameters is fully automated.

In this study, the accuracy of the calculated rate coefficients is assessed by comparing the calculated and experimental rate coefficients. As a measure for the deviation the factor of deviation, ρ, as applied in previous studies,[29,61,62] is defined as follows:

$$\rho = \begin{cases} \dfrac{k_{\mathrm{calc}}}{k_{\mathrm{exp}}} & \text{for } k_{\mathrm{calc}} > k_{\mathrm{exp}} \\ \dfrac{k_{\mathrm{exp}}}{k_{\mathrm{calc}}} & \text{for } k_{\mathrm{exp}} > k_{\mathrm{calc}} \end{cases} \qquad (3)$$

The factor ρ is a value larger then 1 and gives a proper indication for the factor of difference between both rate coefficients. It permits to calculate a mean factor of deviation, $\langle\rho\rangle$, by averaging over a set of reactions which is not possible for the ratio of both rate coefficients.

Group additivity method

The group additivity model for the prediction of activation energies and pre-exponential factors has been described in detail in previous work.[27,29] Briefly, in the group additive model, the rate coefficient is expressed as

$$k = \kappa n_e k_{\mathrm{GA}} = \kappa n_e \tilde{A} \exp\left(-\frac{E_a}{RT}\right) \qquad (4)$$

with κ the tunneling coefficient, n_e the number of single events, $\tilde{A}$ the single-event pre-exponential factor and E_a the activation energy. In the next section, first the group additive modeling of the Arrhenius parameters is presented, followed by the calculation of the number of single events.

In the group additivity method, the transition state is written in terms of Benson groups, see Figure 1. In the Benson method, a group is defined as a polyvalent atom together with all of its ligands. Groups are denoted as X-$(A)_i(B)_j(C)_k(D)_l$ with X the central atom surrounded by i A atoms, j B atoms, k C atoms and l D atoms. To describe the reactions in this work, only hydrogen and carbon atoms are required, but different types of carbon atoms are distinguished however: C_d and C_t for a double respectively triple bound carbon atom, $C^\bullet$ for a radical carbon and

C_B for a carbon atom in a benzene ring. Using Benson groups, the kinetics of hydrogen addition to a broad range of hydrocarbons are then described as perturbations on the kinetics of a reference reaction.

In the transition state depicted in Figure 1, two so-called *primary* groups can be identified, i.e., the group centered on the C_1 and C_2 carbon atoms that are involved in bond formation and breaking. Although the adding hydrogen can, in principle, be regarded as a single-atom primary group it is not considered as a primary group in this work as the adding radical is not varied within the reaction family studied in this work. The groups X_i and Y_i are the *secondary* groups, i.e. those groups having the C_1 or C_2 primary group as a ligand. With these groups the activation enthalpy and activation entropy can be predicted, as the contributions of other groups cancel out between reactants and transition state. Possible steric interactions that cannot be accounted for in the group additive method are considered as *tertiary* contributions. Saeys et al.[27] showed that secondary and tertiary contributions can usually be neglected for carbon-centered radical additions. Due to the small dimensions of the adding hydrogen radical, the error introduced by neglecting secondary and tertiary contributions can be expected to be even smaller for hydrogen than for carbon-centered radical additions. It should however be mentioned that truncation of the group additive method to determine Arrhenius parameters, may lead to deviations between the equilibrium coefficient based on the ratio of forward and reverse reaction coefficient and the equilibrium coefficient based on the thermochemistry of products and reactants. In principle, the construction of the group additive method based on the thermochemistry of the transition state and the reactants leads to built-in thermodynamic consistency, i.e., the difference between the forward and reverse activation energy is related to the reaction enthalpy, and the difference between the forward en reverse pre-exponential factor to the entropy of reaction. However, the neglect of secondary and tertiary contributions for reactants, transition state and products can disturb this thermodynamic consistency, particularly for reactions in which a strong difference in steric and/or resonance effects between reactant and product side is present.[29] Therefore, to assure thermodynamic consistency during the practical application of the group additive method, it is advised to calculate the reverse rate coefficient from the ratio of the forward rate coefficient and the equilibrium coefficient, the latter predicted via thermochemical group additivity for reactants and products.

Extrapolating the common group additivity approximations to hydrogen addition reactions, the activation energy E_a of a given reaction can then be written as function of the primary contributions centered on the C_1 and C_2 carbon atoms:

$$E_a(T) = E_{a,\mathrm{ref}}(T) + \sum_{i=1}^{2} \Delta GAV^{\circ}_{E_a}(\mathrm{C}_i) \qquad (5)$$

In this expression, the activation energy is written as a sum of the reference activation energy $E_{a,\mathrm{ref}}$ and group additive values $\Delta GAV°$. In this notation, Δ denotes the difference between transition state and reactant, while the superscript ° indicates that the values are taken relative to the reference reaction. The applied reference reaction for this reaction family is the addition of a hydrogen radical to ethene, see Figure 2. Hence, the $\Delta GAV°$ in equation 5 pertain to structural differences related to the attacked carbon atom, $\Delta GAV°(C_2)$, and the formed radical, $\Delta GAV°(C_1)$, of a given reaction and the reference reaction as illustrated in Figure 1. The advantage of introducing a reference reaction is that most of the temperature dependence of the Arrhenius parameters can be accounted for by the reference reaction, while the $\Delta GAV°$ are largely temperature-independent.

The single-event pre-exponential factor $\log\tilde{A}$ for a given reaction is expressed as function of the single event pre-exponential factor of the reference reaction $\tilde{A}_{\mathrm{ref}}$ and the primary group additive values $\Delta GAV°$:

$$\log\tilde{A}(T) = \log\tilde{A}_{\mathrm{ref}}(T) + \sum_{i=1}^{2} \Delta GAV^{\circ}_{\tilde{A}}(\mathrm{C}_i) \qquad (6)$$

The practical implementation of the calculation of pre-exponential factors also involves the number of single events n_e, yielding:

$$\log A(T) = \log\tilde{A}_{\mathrm{ref}}(T) + \sum_{i=1}^{2} \Delta GAV^{\circ}_{\tilde{A}}(\mathrm{C}_i) + \log n_e \qquad (7)$$

The number of single events n_e in equation (7) equals:[63-65]

$$n_e = \frac{n_{\mathrm{opt},\ddagger}}{n_{\mathrm{opt},A}\, n_{\mathrm{opt},B}} \frac{\sigma_A\, \sigma_B}{\sigma_\ddagger} \qquad (8)$$

with n_{opt} the number of optical isomers and σ the total symmetry number of the molecule, i.e. the product of the external and the internal symmetry numbers $\sigma_{\mathrm{int},i}$, the symmetry numbers for the internal rotations present.

Most group additive values presented in this work are determined from a single reaction to which only one $\Delta GAV°$ applies. E.g., the $\Delta GAV°$ for the C_1-(C)(H) group is determined from the hydrogen addition to the unsubstituted carbon atom of propene and the reverse β scission. The $\Delta GAV°$ for the activation energy is determined as the difference between the activation energy for the reaction with propene and the reference reaction, i.e. the reaction with ethene. The $\Delta GAV°$ for the pre-exponential factor is determined as the difference of the single event pre-exponential factor with the single-event pre-exponential factor of the reference reaction. Some $\Delta GAV°$ are to be determined from reactions to which multiple groups apply, in particular for additions to triple and allenic bonds. These groups involve the C_{1t}-(C), C_{1t}-(C_d), C_{1t}-(C_t) groups, which always occur in combination with a C_{2t}-(X) group (X=H, C, C_d or C_t), and the $C_{1,\mathrm{alleneII}}$(C)(H) and $C_{1,\mathrm{alleneII}}$-$(C)_2$ group, which always occur together with the $C_{2,\mathrm{allene}}$ group. E.g., the group $C_{1,\mathrm{alleneII}}$-$(C)_2$ is determined from the reaction with 3-methylbuta-1,2-diene:

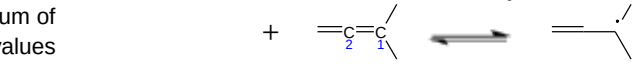

for which the group $C_{2,\mathrm{allene}}$ describes the addition to an allenic carbon atom, and the group $C_{1,\mathrm{alleneII}}$-$(C)_2$ describes the substition at the formed radical.

Tunneling correction

The aim of the group additivity method is the on-the-fly calculation of the rate coefficients of all the reactions in a large radical network, based on a set of available $\Delta GAV°$ for activation energies and pre-exponential factors. As such, its main purpose is to avoid the need of costly quantum chemical calculations in particular for the larger reactions in the network. However, the $\Delta GAV°$ as such do not include quantum mechanical tunneling effects that can be important, in particular at lower temperatures. In general, knowledge of the tunneling contribution for a particular reaction in the reaction network requires knowledge of the energy along the reaction path, and for more accurate treatments even the Hessian, which can be computationally very costly to obtain. Therefore, a method to correct the group additively calculated rate coefficients for quantum mechanical tunneling effects that avoids explicit calculation of the tunneling coefficients for all the reactions present in the reaction network is developed.

As pointed out by Truong,[59] reactions belonging to the same reaction family have the same reactive moiety and are expected to have similarities in their potential energy surface along the reaction path. Therefore, the information on the potential energy surface along the reaction path for the reference reaction, which is usually the "smallest" reaction in the family, can be transferred to the calculation of tunneling contributions to the rate of larger reactions without having to evaluate their tunneling coefficients explicity. In the frame of reaction class transition state theory as developed by Truong,[59] the tunneling contribution to the rate coefficient of a given reaction in the family is determined by multiplying the temperature dependent tunneling coefficient of the reference reaction with a temperature dependent, function:

$$\kappa = \kappa_{\mathrm{ref}}(T)\, f(T) \qquad (9)$$

Truong et al. sucessfully applied this approach to calculate rates for hydrogen abstractions from a limited set of alkanes and alkenes by hydrogen and methyl radicals, using a separate expressions for $f(T)$ for different abstraction sites.[26,60,66,67]

In order to apply expression (9) in the frame of group additivity, a correlation $f(T)$ should be determined for every group or combination of groups. The advantage of the approach of equation (9) is that the tunneling coefficient for the reference reaction can be determined at a higher level, which can be transferred to the other reactions using the correlation for $\kappa/\kappa_{\mathrm{ref}}$. The drawback is that 2 correlations have to be evaluated: a first one expressing the temperature dependence of the tunneling coefficient of the reference reaction and a second one expressing the ratio $\kappa/\kappa_{\mathrm{ref}}$, depending on the groups present in the transition state.

Although a similar procedure can be implemented within the frame of the group additivity method, in this work a more pragmatic approach is investigated to obtain tunneling corrections for reactions belonging to the same family, based on properties that are easily accessible during the practical application of the group additive method. The main factors controlling tunneling in the zero-curvature approximation, i.e. the net electronic tunneling barrier and the imaginary frequency in the transition state, are not accessible during the practical application of the group additive model for rate prediction. However, due to the exothermicity of the hydrogen addition reactions, the addition activation energy provides a good approximation for the net electronic tunneling barrier. Within this approximation, the tunneling contribution to the rate coefficient of a reaction in the family can be expressed as function of the temperature and the activation energy for the addition reaction, $\kappa(T,E_{a,\mathrm{add}})$. The advantage of this approach is that tunneling corrections for all reactions for which $\Delta GAV°$ are available can be modeled very easily. In this work, an appropriate expression for $\kappa(T, E_{a,\mathrm{add}})$ is derived. The results of this approach and that using approach of expression (9) are compared.

Results and Discussion

In this section, first the reliability of the computational method is illustrated by comparison with high-level quantum chemical data available in literature and with experimental values. Next, the rate coefficients are presented and the activation energies and pre-exponential factors, which are derived from an Arrhenius fit to the ab initio calculated rate coefficients, i.e. without tunneling contributions, are discussed. Then, the group additive values are presented and an expression to account for tunneling effects is derived. Finally, the use of the group additive model is illustrated and validated by comparing the predictions with ab initio calculated values and with experimental rate coefficients.

Validation of the computational method

Previous level of theory studies showed that the CBS-QB3 method yields accurate data for similar radical reactions. In this section, the reliability of the CBS-QB3 method for hydrogen addition reactions is illustrated. Table 1 provides a comparison of the CBS-QB3 data with the QCISD(T) quantum chemical data, extrapolated to the infinite basis-set limit, as reported by Miller and Klippenstein,[44,45] for the activation energy barriers at 0 K, $\Delta E(0\ \mathrm{K})$, the reaction energies at 0 K, $\Delta_r E(0\ \mathrm{K})$, and high-pressure limit rate coefficients of the reactions H + ethene, ethyne and 1,3-butadiyne. The CBS-QB3 barriers are systematically lower than the QCISD(T)/∞ values by 1-3 kJ mol^{-1}, but for the largest deviation of 2.8 kJ mol^{-1} for the addition to 1,3-butadiyne, Klippenstein and Miller had to reduce the barrier by 2.1 kJ mol^{-1} in order to bring the rate coefficient in agreement with experimental measurements.[68] The reaction energies are also lower by 1 to 4 kJ mol^{-1}, except for the addition to ethene. Due to the lower CBS-QB3 barriers, the CBS-QB3 rate coefficients are slightly larger than the QCISD(T)/∞ values, by 10 to 70% for the addition to ethene and ethyne, and up to a factor 3 at 300 K for the addition to 1,3-butadiyne. All differences between the rate coefficients can be attributed to the differences in the reaction barrier. Miller and Klippenstein had already indicated variational effects to be small for these reactions (max. 15% at 2500 K). Summarizing, the CBS-QB3 results in this paper agree well with other high-level calculations from literature.

In Table 2 rate coefficients obtained using CBS-QB3 are compared to experimental rate coefficients taken from the NIST Chemical Kinetics Database,[69] when available. The set of experimental reference data includes only data indicated by NIST as 'Absolute rate value measured directly', 'Experimental value and limited review', 'Derived from detailed balance/reverse rate' and 'Extensive literature review'. For the latter category values indicated to be an estimation were excluded. This yielded 7

reactions for which the calculations could be compared to experimental reference data at 300, 600 and 1000 K, see Table 2. The experimental references and respective rate coefficients for these 7 reactions are given in Table S1 of the Supporting Information. The deviation ratios k_{calc}/k_{exp} and the factor of deviation ρ for each experimental reference can be retrieved in Tables S2-S3 of the Supporting Information while the mean factors of deviation <ρ> averaged per reaction are shown in Table 2.

From Table 2 it is clear that, also for hydrogen additions and β scission, the CBS-QB3 method performs very good. For additions, the reaction-averaged factors of deviation <ρ> are smaller than 3 for all reactions. For β scissions, a deviation larger than 3 is only observed for the β scission of a primary propyl radical to propene (reaction 3), mainly due to the deviation from the 600 K experimental reference of Mintz.,[70] and for the β scission of a *tert*-butyl radical yielding isobutene (reaction 7).

The mean factor of deviation averaged out for the different temperatures and reactions is 1.7 for the additions and 2.1 for the β scissions, yielding a value of 1.9 on average for this reaction family. Hence, for hydrogen additions, the CBS-QB3 approach yields even better results than for other reaction families. For carbon-centered radical addition[62] a mean factor of deviation of 3 was found, while for hydrogen abstractions[61] a mean factor of difference of 5.8 was found, the latter however mainly determined by large deviations at 300 K.

Rate coefficients

The rate coefficients including tunneling contributions at 300 K for hydrogen additions and β scissions evaluating the influence of substituents at C_1 can be found in Table 3 and for the reactions evaluating the influence of substituents at the C_2 carbon atom in Table 4. Kinetic parameters at 600 and 1000 K, as well as the parameters characterizing the transition state, applied symmetry numbers, number of optical isomers and number of single events can be found in Supporting Information Tables S4-S6. The transition state geometries are reported at the end of the Supporting Information.

The resulting rate coefficients for additions range from 10^2 to 10^7 m^3 mol^{-1} s^{-1} at 300 K. The reactions evaluating the influence at C_1 are much faster than the second set in which the substituents on the C_2 carbon atom are varied, in agreement with the findings that the unsubstituted carbon is the kinetically most favorable site for radical attack.[41] The fastest reactions are the additions to the terminal carbon atom of 1,3-butadiene compounds (reactions 4-6); the slowest reaction is the addition to the phenyl substituted carbon atom of styrene yielding the 2-phenyleth-1-yl radical (reaction 28).

For β scissions, with rate coefficients ranging from 10^{-32} to 10^{-9} s^{-1} at 300 K, the kinetics are dominated by the strong endothermicity for these reactions. The slowest reaction is the β scission of the 3-methylbut-1-en-3-yl radical into 3-methylbuta-1,2-diene (reaction 15), as the formation of allenic moieties from allylic radicals are the most endothermic reaction of the whole set. The fastest reaction is the formation of the resonance-stabilized 2-ethynylbuta-1,3-diene (reaction 26), which is the least endothermic reaction. Clearly, the rates of the strongly endothermic β scissions are determined primarily by the reaction enthalpy.

Despite the very light hydrogen atom, the influence of tunneling on the rate coefficients is rather small due to the very low tunneling barriers. The tunneling coefficients for the reactions of Tables 3 and 4 range between 0.49 and 2.7 at 300 K. For two reactions reflection occurs: the hydrogen addition to 2-methylbuta-1,3-diene (reaction 5) and the addition to 2-ethynylbuta-1,3-diene (reaction 9) are almost barrierless with an extremely low electronic barrier of 0.6 kJ mol^{-1} and 0.1 kJ mol^{-1}. For the barrierless addition to 2-ethenylbuta-1,3-diene (reaction 6) no transmission coefficient was accounted for due to convergence problems, though reflection can be expected.[71] Despite the small corrections, tunneling coefficients should definitely be accounted for below 500 K since the effects are larger than 50%. For temperatures of 500 K and higher, the contribution of tunneling is limited to 50% and at 1000 K the largest tunneling coefficient reduces to a negligible 1.08.

Arrhenius parameters

The Arrhenius parameters at 300 K are given in Table 3 for the reactions evaluating the influence of substituents at C_1, and in Table 4 for the reactions evaluating the influence of substituents at the C_2 carbon atom. The reported Arrhenius parameters have been fitted to the ab initio calculated rate coefficients without tunneling contributions. In this section first the pre-exponential factors and activation energies for addition are discussed, followed by the β scissions.

For additions to the terminal C_2 carbon atom, in which the substituents at the C_1 carbon atom are varied (Table 3), the pre-exponential factors $\log(A/m^3\ mol^{-1}\ s^{-1})$ range between 6.7 and 8.1, the lowest value pertaining to the addition to styrene (reaction 11) and the highest to the addition to the linear 1,3-butadiyne (reaction 18). The substituents at the C_1 carbon atom have little effect on the pre-exponential factor for addition, except for additions to triple bonds for which an increased pre-exponential factor is observed. The activation energies for the additions of Table 3 range between 0 and 15 kJ mol^{-1}. Many of the reactions have very low activation energies as the C_1 substituents stabilize the formed radical by resonance and/or hyperconjugation lowering the activation energy. The addition to 2-ethenylbuta-1,3-diene (reaction 6) forming a strongly resonance-stabilized radical is found to be barrierless.

For additions in which the substituents on the attacked C_2 carbon atom are varied (Table 4) the rate-decreasing effect of the substituents is reflected in a decrease in the pre-exponential factor and an increase in the activation energy as compared to the additions to the unsubstituted end from Table 3. The only exceptions are the additions to triple bonds, in particular the H addition to ethyne and 1,3-butadiyne for which pre-exponential factors are about an order of magnitude higher than the other values. For these reactions, the molecular linearity is lost upon transition state formation resulting in a larger activation entropy. The activation energies range between 15 and 28 kJ mol^{-1}, which is about 15 kJ mol^{-1} higher than for the additions to the unsubstituted carbon atom which is mainly due to a reduced stabilization of the forming radical and an increased steric hindrance in the transition state.

Reactivity patterns in radical reactions are frequently described using an Evans-Polanyi relationship that correlates the activation energy with the reaction enthalpy for a set of homologous reactions. An Evans-Polanyi plot of the activation energy versus the reaction enthalpy at 300K is presented in Figure 3 for the additions reactions with varying substituents at C_1 (Table 3). Figure 4 presents this correlation for the addition reactions with varying substituents at C_2 (Table 4). From these figures, it can be seen that, next to the reaction enthalpy, other factors also play a role in determining the activation energy. As pointed out by Clarke et al.,[43] there is a significant contribution of charge transfer states, in particular of the ionic state formed by transferring electron density from the alkene, to the barrier of hydrogen additions. Fischer and Radom[41] propose to describe the effect of charge transfer states on the activation energy of addition reactions by using polar factors:

$$E_a = E_{a,enth} F = (E_a^o + \gamma \Delta_r H^\circ) F_n F_e \qquad (10)$$

In this expression, the enthalpic contribution to the activation energy is determined from an Evans-Polanyi plot that describes the upper-bound to the set of data points, i.e. the line through the points for reactions 6 and 11 (Table 3) in Figure 3 and through the points for reactions 1 and 27 (Table 4) in Figure 4. In the latter data set, the points corresponding to the additions to styrene and triple bonds have been omitted to determine the enthalpic contribution as these reactions clearly have a somewhat different behavior than the other reactions in the set. The electrophilic factor, F_e, as defined by Fisher and Radom,[41] depends on the difference between the electron affinity of the radical and the ionization energy of the alkene and describes the influence on the activation energy of charge transfer states formed by transferring electron density from the alkene to attacking radical. Its nucleophilic counterpart, F_n, depends on the difference between the ionization energy of the radical and the electron affinity of the alkene and describes the influence of charge transfer states formed by transferring electron density from the attacking radical to the alkene. These differences are calculated based on the vertical ionization energies, E_i, and electron affinities, E_{ea}, of the alkenes and the hydrogen radical. These values have been calculated at the B3LYP/6-311G(d,p) level of theory and can be found in Table S7 of the Supporting Information. The behavior of the polar factor, *F*, versus the energy of the charge separated configurations allows evaluating the nature of the polar influence. In contrast to the variation of adding radicals for carbon-centered radical additions,[29] there is no correlation found between the expected nucleophilicity ($E_{i,\mathrm{H}} - E_{ea,\mathrm{alkene}}$) and the polar factor *F*. As illustrated in Figures 5 and 6, the expected electrophilicity ($E_{i,\mathrm{alkene}} - E_{ea,\mathrm{H}}$) correlates with the polar factor *F* for both sets of hydrogen additions reactions in accordance with the charge transfer to the hydrogen radical in the transition state as identified by Clarke et al.[43] In general, the electrophilic influence is much smaller for the hydrogen addition to the substituted C_2 atom (Table 4) than for the addition to the unsubstituted C_2 atom, but a quantitative correlation of this effect that is valid for all of the reactions in Tables 3 and 4 is not straightforward. Similar observations concerning the use of a combination of an Evans-Polanyi relation and polar factors describing the reactivity trends in carbon radical centered radical additions have been made previously for carbon-centered radical additions.[29]

For the β scissions in which the substituents at the forming radical center are varied (see Table 3), the values for $\log(A/s^{-1})$ vary between 12.2 and 14.1, resp. for the β scission yielding 2-ethynylbut-1-en-3-yne (reaction 10) and the β scission forming 1,2-butadiene (reaction 14). The presence of substituents at the forming radical center increases the pre-exponential factor for β scission; all but 2 reactions from Table 3 have a larger pre-exponential factor than the β scission of the unsubstituted ethyl radical. The activation energies are very large for this reaction family, up to 258 kJ mol^{-1} for the β scission of a secondary allylic radical forming 1,2-butadiene (reaction 14). For these reactions, the activation energies are clearly dominated by the strong endothermicity. Only exceptions are the activation energies for the β-scission reactions yielding propene (reaction 2) and isobutene (reaction 3), which are lower than the activation energy of the β scission forming ethene (reaction 1) while the reaction enthalpy remains about the same. The same holds for the addition reactions, for which the activation energies for these reactions are lower than for the addition to ethene. Apparently, the methyl substituents present in these reactions stabilize the transition state more than the radical.

Finally, the effect on the β scission kinetics of substituents on the C_2 carbon atom (see Table 4) is discussed. These substituents have only a small effect on the pre-exponential factor with most log*A* values similar to the β scission of the ethyl radical ($\log(A/s^{-1})$ = 12.3-13.1), except for β scissions yielding allenic and triple bonds (reactions 30-34), for which $\log(A/s^{-1})$ ranges from 13.3 to 14. Also with exception of the β scissions yielding allene and triple bonds, the activation energies range between 126 and 152 kJ mol^{-1}. In general, the substituents at the C_2 atom result in an increase of the activation energy as opposed to their effect on the addition path where the substituents on the C_2 atom decrease the rates. The C_2 substituents stabilize the formed alkene more than the radical, which decreases the β scission activation energy with respect to the β scission yielding ethene. For the β scissions yielding allene and triple bonds higher activation energies occur, up to 257 kJ mol^{-1} for the decomposition of an allylic radical to allene (reaction 30).

The difference in behavior between β scissions yielding triple bonds and the β scissions yielding alkenes can be understood as follows. For the β scissions forming alkenes the π bond formation involves the transition from a single to a double bond, and the double bond formation strongly reduces the internal mobility in the transition state relative to the product radical. The transition state is late from a β-scission viewpoint, which means that the rotation about the forming π bond is already severely inhibited. For the formation of triple bonds through β scission of a vinylic radical that already contains a double bond there is no loss in mobility due to increased hindrance of rotation around the forming bond. Also, the presence of several low frequency modes indicate an increase in mobility in proceeding from the vinylic radical to the transition state. The increase in mobility upon transition state formation results in a higher pre-exponential factor than for the β-scission reactions yielding alkenes. Albeit to a lesser extent, this is also the case for the β scission of resonance-stabilized radicals, due to the additional constraints on the internal mobility of the radical imposed by the resonance. A very pronounced case is the β scission of an allyl radical with the formation of allene (reaction 30), for which the pre-exponential factor for β scission is 2 orders of magnitude higher than for the β scission of the ethyl radical

yielding ethene. In this reaction, not only does the allyl radical have a low entropy due to the resonance stabilization but, moreover, the transition state has a large vibrational contribution to the entropy. The internal mobility of the transition state is enhanced upon formation of the transition state since formation of the allenic C=C=C moiety requires that the resonant allyl π system be broken in going from reactant to transition state as illustrated in Figure 7. The vibrational activation entropy for this β scission is some +15 J mol^{-1} K^{-1} as compared to −9 J mol^{-1} K^{-1} for the vibrational activation entropy of the reference β scission of the ethyl radical.

Group additive values

The group additive values Δ*GAV*° are determined from the Arrhenius parameters of 34 reactions given in Tables 3 and 4. All Δ*GAV*° are determined from a single reaction.

In Table 5 the resulting group additive values are given for 300 and 1000 K. Group additive values at 600 K can be found in Table S8 of the Supporting Information. The single event Arrhenius parameters for the reference reaction are given in Table 6 for temperatures between 300 and 1300 K.

A closer look at the group additive values in Table 5 provides a clear view on the effect of substituents on the C_1 and C_2 carbon on the kinetics. Most Δ*GAV*°(C_1) relate to a stabilization of the product radical with respect to the reference reaction, and hence the group additive values for the addition activation energy are negative while those for β scission are strongly positive. The β-scission activation energy increases up to 75 kJ mol^{-1} for the diallylic radical group C_1-(C_d)$_2$ (group C_1-5). The substituents at the C_1 carbon atom have little effect on the pre-exponential factor for addition, as discussed previously. For β scission, the Δ*GAV*° for pre-exponential factors are generally positive, partially compensating the effect of E_a on the kinetics.

The group additive values accounting for the influence of substitution at the attacked C_2 carbon atom, Δ*GAV*°(C_2), have a strong rate-decreasing effect on addition through a combination of a decrease in the pre-exponential factor and an increase in the activation energy. There are 2 exceptions: the C_{2t}-(H) and C_{2t}-(C_t) group (resp. C_2-13 and 16) have a large positive contribution to log*A*. These Δ*GAV*° have been determined from the hydrogen addition to the linear molecules ethyne and buta-1,3-diyne discussed above. For β scissions, the contributions of substituents on the C_2 carbon atom increase the rate coefficient. As discussed above, the substituents on C_2 stabilize the formed alkene more than the radical leading to the negative Δ*GAV*° for the β scission activation energies. Contributions to the log*A* for β scissions are generally slightly positive, adding to the rate-increasing character of the *ΔGAV*° for E_a. Exceptions to these general trends for the C_2 contributions to the β scission rate coefficients are the reactions involving triple bonds and allene (groups C_2-12 to 16) for which the *ΔGAV*° is positive for E_a and strongly positive for log*A*, up to *ΔGAV*°(log*A*) = 2, due to the increase in mobility on transition state formation as compared to the reference reaction.

As illustrated in Figure 8, the temperature dependence of the Δ*GAV*° is limited in the range 300-1300K. For addition reactions, the Δ*GAV*° vary by less than 1 kJ mol^{-1} on the activation energy and 0.1 on the pre-exponential factor for all but 4 groups, see Figure 8. For β scission, the temperature dependence is somewhat larger but remains limited to 3 kJ mol^{-1} on the activation energy and to 0.34 on the pre-exponential factor. Compared to the temperature dependence of the actual Arrhenius parameter in this temperature range, between +0.5 and +1.0 for log*A* and +7 to +12 kJ mol^{-1} for E_a, this is small, indicating that most of the temperature dependence of the kinetic parameters is indeed accounted for by the $E_a(T)$ and log$A(T)$ of the reference reaction. The larger temperature dependences for addition are observed for the Δ*GAV*° for the C_{1t}-(C), C_{1t}-(C_d), C_{2t}-(H) and C_{2t}-(C_t), group, for which the Δ*GAV*° for E_a vary with about 4 kJ mol^{-1} between 300 and 1300 K. The increased temperature dependence is again related to the linearity of the reactants ethyne and buta-1,3-diyne from which the Δ*GAV*° for resp. the C_{2t}-(H) and C_{2t}-(C_t) group have been derived. The temperature dependence of the additional vibration in the linear molecule ($C_p \cong R$) is larger than for the lost external rotational degree of freedom ($C_p = R/2$), which explains the decrease in Δ*GAV*° with temperature. The Δ*GAV*° for the other 2 groups, C_{1t}-(C) and C_{1t}-(C_d), are derived from the hydrogen additions to propyne and but-1-en-3-yne. These reactants are not linear, but since these reactions also involve the C_{2t}-(H) group, the Δ*GAV*° for the C_{1t}-(C) and C_{1t}-(C_d) groups have the inverse temperature dependence and increase with temperature. In the temperature range of 1000 K however, a change of 4 kJ mol^{-1} can still be considered acceptable. In most applications the kinetics are required in a much narrower temperature range. Moreover, the positive correlation between the variation with temperature of both Arrhenius parameters limits the deviations on the rate coefficients to a factor of 3 for all groups, even if 300 K Δ*GAV*° are used at 1300 K and vice versa. When the 4 C_t groups are excluded, the deviations on the rate coefficient are even limited to a factor of 2.

From the discussions above, it is clear that the addition to triple and allenic bonds show a different behavior then the addition to double bonds. This different behavior is also reflected in the magnitude and temperature dependence of their group additive values. Although their inclusion in the same reaction family is questionable, the differentiation between C_d and C_t carbon atoms made in the group additive method allows the description of their kinetics. As such, the groups describing additions to triple bonds can be seen to form a subset including all groups centered on a C_t atom, thus enabling the inclusion of addition to double and triple bonds in the same reaction family and using the same reference reaction.

Tunneling correction

As discussed in section 0, the Δ*GAV*° reported in Table 5 do not include contributions of quantum mechanical tunneling effects. However, as shown above, an accurate description of the kinetics for the hydrogen addition/β scission reactions requires inclusion of tunneling effects since these are significant at temperatures below 400 K. In this section, an approach is presented to obtain tunneling corrections for the reactions belonging to the hydrogen addition/β-scission family as function of the temperature and activation energy for the addition reaction, $\kappa(T,E_{a,add}(T))$. This approach allows an easy determination of tunneling corrections for all reactions to which the group additivity model presented in this paper applies. Note that $E_{a,add}(T)$ pertains to the addition

activation energy that can be predicted using the group additive values presented above, taken at the appropriate temperature.

Figure 9 presents the correlation between the Eckhart tunneling coefficients with the addition activation energies for the reactions in Tables 3 and 4. At 300 K, the tunneling coefficients range between 0.5 and 2.7. Because of the presence of reflection at low barriers, a power law provides the best description of the tunneling behavior. Expression (11) was obtained by regression of tunneling coefficients in the range 300-1000 K (see Table S9 of the Supporting Information) to the activation energies at the respective temperatures:

$$\kappa(T, E_{a,\mathrm{add}(T)}) = 0.84\left(E_{a,\mathrm{addition}}\right)^{\frac{56}{T-120}} \qquad (11)$$

In this equation, $E_{a,\mathrm{add}}(T)$ has dimensions kJ mol^{-1} while T is expressed in K. The excellent agreement, shown in Figure 9, yields a mean $\langle\rho\rangle$ of only 1.07 between the power-law predicted and the Eckart tunneling coefficient at 300 K. The largest deviation is an acceptable factor of 1.2. At higher temperatures, the average deviations decrease. The remaining deviations are function of the imaginary frequency, which is however not accessible during group additivity predictions. It should be mentioned that correction for tunneling contributions is important at temperatures up to 400 K only. For temperatures of 500 K and higher, tunneling has only a marginal contribution and can thus be neglected.

An alternative correlation expressing the tunneling coefficient as function of the reference reaction's tunneling coefficient, in line with the approach of Truong et al. for hydrogen abstractions as discussed in the methodology section,[26,60,66,67] is given in Supporting Information.

Application and validation of the method

In this section, first the application of the group additive method for the calculation of the Arrhenius parameters is illustrated. Next, the obtained group additive model is validated by comparing group additive predictions to (i) 11 ab initio calculated rate coefficients for addition to various types of unsaturated hydrocarbons (see Tables 7-8) and (ii) 7 experimental rate coefficients (see Table 9).

To obtain the pre-exponential factor and activation energy for the hydrogen addition to trans-2-butene (reaction 1a in Table 7), for instance, the required $\Delta GAV°$ are the C_1-(C)(H) and C_2-(C)(H) groups pertaining to the methyl substituents on the C_1 and the C_2 carbon atom. At 1000 K, the activation energy for this addition can be written as

$$E_a(1000\ \mathrm{K}) = E_{a,\mathrm{ref}} + \Delta GAV^{\circ}_{\mathrm{Ea}}\ [C_1\text{–}(C)(H)] + \Delta GAV^{\circ}_{\mathrm{Ea}}\ [C_2\text{–}(C)(H)]$$

$$= 18.5 - 2.4 + 4.0 = 20.1\ \mathrm{kJ\ mol^{-1}}$$

while the ab initio calculated activation energy amounts to 18.9 kJ mol^{-1}, an overestimation of only 1.2 kJ mol^{-1}. Similarly, at 1000 K, the β scission activation energy can be calculated to be 152.7 kJ mol^{-1}, which is only 0.6 kJ mol^{-1} lower than the ab initio calculated activation energy. The calculation of the pre-exponential factor requires the number of single events to be determined. For the reactant trans-2-butene, the external symmetry number is 2 and the internal symmetry number is $3^2 = 9$. For hydrogen σ = 1. The transition state has no external symmetry but still possesses the 9-fold internal symmetry and exhibits molecular chirality, i.e., $n_{\mathrm{opt}} = 2$. With these values, the number of single events for addition can be written as:

$$n_e = \frac{n_{\mathrm{opt},\ddagger}}{\prod_j n_{\mathrm{opt},j}} \frac{\prod_j \sigma_j}{\sigma_\ddagger} = \frac{2}{(1\cdot1)} \frac{(1\cdot1)(2\cdot9)}{1\cdot9} = 4$$

The pre-exponential factor can then be calculated as:

$$\log(A(1000\ \mathrm{K})/\mathrm{m^3\ mol^{-1}\ s^{-1}}) = \log\tilde{A}_{\mathrm{ref}} + \Delta GAV^{\circ}_{\log\tilde{A}}\ [C_1\text{–}(C)(H)] + \Delta GAV^{\circ}_{\log\tilde{A}}\ [C_2\text{–}(C)(H)] + \log n_e$$

$$= 7.726 + 0.019 - 0.217 + \log 4 = 8.130$$

which agrees very well with the ab initio calculated $\log(A/\mathrm{m^3\ mol^{-1}\ s^{-1}})$ of 8.158. For the reverse reaction, with a number of single events of 2, $\log(A/\mathrm{m^3\ mol^{-1}\ s^{-1}})$ amounts to 13.580 as determined by group additivity, which is only 0.072 off of the ab initio value. At 1000K, tunneling corrections can be neglected resulting in a rate coefficient of 1.2 10^7 m^3 mol^{-1} s^{-1} for addition, and 4.0 10^5 s^{-1} for β scission, which are both within 30% of the respective ab initio calculated rate coefficients of 1.5 10^7 m^3 mol^{-1} s^{-1} and 3.1 10^5 s^{-1}.

To obtain the kinetic parameters for this same addition at 300 K, the Arrhenius parameters for the reference reaction and the $\Delta GAV°$ at 300 K are used yielding:

$$E_a(300\ \mathrm{K}) = 10.4 - 2.4 + 4.3 = 12.3\ \mathrm{kJ\ mol^{-1}}$$

$$\log A(300\ \mathrm{K}) = 7.010 + 0.017 - 0.188 + \log 4 = 7.441\ \mathrm{m^3\ mol^{-1}\ s^{-1}}$$

At 300 K tunneling correction is relevant and the tunneling coefficient $\kappa(T, E_{a,\mathrm{add}}(T))$ can be obtained as

$$\kappa(T, E_a) = 0.84\left(E_{a,\mathrm{addition}}\right)^{\frac{56}{T-120}} = 0.84\left(12.3\ \mathrm{kJ\ mol^{-1}}\right)^{\frac{56}{300\mathrm{K}-120}} = 1.83$$

Using these values, the rate coefficient at 300 K is found as

$$k(300\,\mathrm{K}) = 1.83\,10^{7.441}\exp\left(-\frac{12.3\,\mathrm{kJmol^{-1}}}{RT}\right) = 3.6\,10^5\ \mathrm{m^3 mol^{-1} s^{-1}}$$

which is within 40% of the ab initio determined (tunneling corrected) value of 5.8 10^5 m^3 mol^{-1} s^{-1}.

Ab initio validation

To validate the group additive method, the group additively predicted rate coefficients are compared to ab initio calculated rate coefficients for 11 hydrogen additions (see Tables 7-8) to unsaturated hydrocarbons ranging from butenes to strongly resonance-stabilized species such as 1,3,5-hexatriene and to allenic and triple bonds. The test reactions also include species for which a deviation from the truncated group additive model is expected such as addition to 2,3-dimethylbut-2-ene which suffers greatly from steric effects. Differences between ab initio calculated and group additive predicted Arrhenius parameters and tunneling coefficients can be found in Table 7 while differences in rate coefficients and equilibrium coefficients are presented in Table 8. The actual calculated and predicted values, the number of single events and the parameters characterizing the transition state are given in Tables S10-S12 of the Supporting Information. The group additive predictions use the $\Delta GAV°$ at the indicated temperature.

The tunneling coefficients at 300 K are predicted excellently by Eq. (11), the largest deviations being 14%. The ratio between the predicted an ab initio pre-exponential factor is between 0.6 and 5 at 300 K, the largest deviations are observed for reactions 5 and 11. For activation energies, the mean absolute deviation between prediction and ab initio calculation amounts to 2.3 kJ mol^{-1}, with deviations ranging between −12.5 and 6.5 kJ mol^{-1} (for reactions 5β and 11β). The deviations at 1000 K are similar to those at 300 K.

Reaction 5, the hydrogen addition to 2,3-dimethylbut-2-ene, which has deliberately be included since the the strong steric effects present in this reaction will bias the group additive prediction, indeed shows the largest deviation on the activation energy. In the reactant alkene, a double cis interaction is present as illustrated in Figure 10. In the transition state, this cis strain is partially released due to the formation of the sp^3 centre. As the truncated group additive method contains only primary contributions, the partial release of the cis strain in going from the alkene to the transition state is not accounted for resulting in an overestimation of the activation energy of the forward addition by 5.3 kJ mol^{-1}. For the reverse β scission of the 2,3-dimethylbut-2-yl radical, an increased steric interaction is caused by the developing cis interaction in the transition state for formation of the 2,3-dimethylbutene, leading to an underestimation of the activation energy of 12.5 kJ mol^{-1}. In the truncated group additive method, the groups centered on the C_1 and C_2 carbon atom are considered independent from each other. As a consequence, the mutual strain caused by the simultaneous presence of substituents on C_1 and C_2 cannot be accounted for by the truncated group additive method as it does not include the tertiary contributions that are required to properly account for this effect. For this β scission, the neglected mutual strain is larger in the transition state than in the reactant radical, where gauche interactions but no cis interactions are present. It can be shown quantitatively that the deviation on the activation energy for this β scission is caused by the cis interaction. The double cis interaction as present in 2,3-dimethylbutene has a contribution of 18.3 kJ mol^{-1} to the standard enthalpy of formation,[72] while the steric interaction of the 2 radical gauche interactions (type 1) in the product radical involves a gauche correction of 5.4 kJ mol^{-1}.[72] As the transition state for β scission is very late, it can be assumed that the cis interaction is almost entirely developed in the transition state. Therefore, the neglected change in steric effect on the activation energy can be estimated to be about 18.3 – 5.4 = 12.9 kJ mol^{-1}, which corresponds very well with the observed difference of 12.5 kJ mol^{-1} between group additive and ab initio activation energy. The same reasoning holds for the β scission of the but-2-yl radical forming cis-2-butene (reaction 2b). The activation energy is underpredicted by 5.7 kJ mol^{-1} agreeing very well with the cis contribution to the standard enthalpy of formation of 5.9 kJ mol^{-1}.[72]

For all reactions except those with strong steric interactions in the reactants (reactions 2β and 5β, see Table 8), the group additive predicted rate coefficients at 300 K are within a factor 3.5 of the ab initio predicted value. As discussed above, most troublesome is reaction 5β, for which the deviation of 12 kJ mol^{-1} on the β scission activation energy causes the rate to be underestimated by a factor of 160 at 300 K. The addition rate coefficient for reaction 5a remains within a factor of 2. The second largest deviation is the overprediction by a factor of 8 for the β scission of the but-2-yl radical (reaction 2), again caused by a cis interaction in the transition state. A parity plot of the group additive rate coefficients vs. the ab initio calculated values is given in Figure 11. The mean factors of deviation <ρ> are 1.6 for addition and, due to the large deviation for reaction 5β, 17 for β scission. Removing this outlier, the <ρ> value for β scission drops to 2.7.

At 1000 K, the largest deviation on the rate coefficient is reduced to a factor 4 for the β scission of the 2,3-dimethylbut-2-yl radical (reaction 5β). For all other reactions, the deviations are smaller than a factor 2.5; for 75% of the reactions even smaller than a factor 1.5, which can be considered an excellent agreement between prediction and ab initio calculation. The averaged mean factors of deviation <ρ> are 1.5 for addition and 1.7 for β scission.

From these results, it can be concluded that the truncated group additive method yields accurate predictions provided that no strong steric effects influence the kinetics. This is due to the neglect of tertiary contributions in the truncated group additive model which is restricted to primary effects, i.e., to the groups centered on the C_1 and C_2 carbon atom. These tertiary contributions, originating from non-nearest neighbor interactions, are already difficult to model for thermodynamics and modeling these interactions for kinetics is expected to be even more troublesome.[72] The neglect of tertiary contributions however does not have significant effects on the accuracy of the rate coefficients for addition. Therefore, for reactions with severe steric effects, it is suggested to calculate the β scission rate coefficient from the addition rate coefficient and the thermodynamic equilibrium coefficient. And since accurate equilibrium coefficients are of primary importance for use in reaction networks, best results will be obtained by calculating the β-scission rate coefficient from the addition rate and the equilibrium coefficient for all reactions, implementing thermodynamic consistency explicitly. The thermodynamic equilibrium can be calculated using thermochemical group additivity, which predicts equilibrium coefficients more reliably, typically within a factor of 2.[73]

Based on the reactions of Table 7, the group additive method outperforms models such as Evans-Polanyi correlations.[15,16] Applying an Evans-Polanyi relation obtained from the reactions in Tables 3 and 4 for the prediction of the 300 K activation energies of Table 7, an average overestimation of the ab initio activation energies of 4.3 kJ mol^{-1} is found, compared to an overestimation by 1.3 kJ mol^{-1} for the group additive method (see Figures S1-S2 in Supporting Information). Group additivity clearly improves the agreement with the ab initio activation energy, and the method is moreover capable of predicting pre-exponential factors in contrast to the Evans-Polanyi method.

Experimental validation

In this section, the group additive predicted rate coefficients are compared to experimentally determined rate coefficients at 300, 600 and 1000 K (see Table 9). The 7 reactions all involve hydrogen addition/β scission data available on NIST Chemical Kinetics Database[69] that have not been used previously for the validation of the computational method. From the 16 addition rate coefficients in the 300 K category, 10 have been determined at 296, 298 or 303 K. For the sake of conciseness, we included these rate coefficients in the 300 K category.

In Table 9 the ρ values averaged per reaction are given. The actual experimental rate coefficients are given in Supporting Information Table S13, and the individual deviation ratios and ρ values in Tables S14-S15. For 4 of the 7 reactions in Table 9, the ρ values are smaller than a factor 3 at all temperatures. At the 600 and 1000 K, all deviations are smaller than a factor 3 while the larger deviations are observed at 300 K indicating that the deviations are most possibly related to differences in the activation energy. The largest deviation occurs for the β scission of the but-2-yl radical forming 1-butene (reaction 4), with a <ρ> value of 8.2 at 300 K. Averaged over all reactions and over the temperatures 300-1000K, a mean factor of deviation <ρ> of 2.0 is found, indicating an excellent agreement between the group additive method and the experimental rate coefficients for this reaction family. It should be noted that this mean factor of deviation of 2 mainly originates from the mean factor of deviation between the CBS-QB3 calculated values and experiment, for which a <ρ> value of 1.9 was obtained in section 0.

Conclusion

This study provides a group additive model for the kinetics of hydrogen addition. The applied model is an extension of the previously published group additive method for carbon-centered radical additions,[29] and allows the prediction of hydrogen addition and β-scission rate coefficients to a wide range of unsaturated hydrocarbons.

The rate coefficients are calculated using Conventional Transition State theory based upon ab initio CBS-QB3 calculations, with Eckart tunneling corrections. This computational approach is validated with experimental data on a set of 7 reactions, for which a mean factor of deviation of only 1.9 is found in the temperature range 300-1000 K.

From CBS-QB3 calculated Arrhenius parameters a set group additive values Δ*GAV*° for activation energies and pre-exponential factors is derived. The temperature dependence of these Δ*GAV*° is, except for four C_{1t}-centered groups, very low. Therefore, a set of Δ*GAV*° at a single temperature is sufficient to describe the kinetics, even for a process with wide temperature ranges. Tunneling, which is significant at 400 K and lower, is modeled separately since it cannot be incorporated into the additivity method. A power law correlation between the tunneling coefficients and the activation energy for addition, the latter being predicted using group additivity, successfully describes the tunneling coefficients.

The obtained group additive model is validated by comparing predicted rate coefficients with ab initio calculated rates for 11 reactions. The rate coefficients are predicted well, except for reactions with strong steric effects such as addition to 2,3-dimethylbut-2-ene. For additions, the mean factor of deviation between prediction an ab initio rate coefficient is 1.6 at 300 K and 1.5 at 1000 K. For β scissions, the agreement is less since steric effects contribute more to the rate, which also leads to inaccurate predictions of the equilibrium coefficients. Therefore, calculation of the β-scission rate coefficients from the addition rates and the thermodynamic equilibrium is advised.

Further comparison of predicted with experimental data for 7 reactions in the range 300-1000 K yields a mean factor of deviation of 2.0, which is of the same magnitude as the performance of the CBS-QB3 method in comparison with experimental rate coefficients. Hence, the presented group additive method can be reliably applied to predict hydrogen radical addition rate coefficients with a reasonable accuracy in the whole temperature range 300-1000 K.

Acknowledgements

M.K.S. held a Ph.D. grant of the Institute for the Promotion of Innovation through Science and Technology in Flanders (IWT-Vlaanderen) and is grateful for financial support from the Fund for Scientific Research-Flanders (F.W.O.-Vlaanderen)

Keywords: gas phase kinetics · group additivity · ab initio kinetics · radical reactions

[1] H. Z. R. Zhang, E. G. Eddings, A. F. Sarofim, *Energy & Fuels* **2007,** *21* (2), 677-685.
[2] E. Ranzi, M. Dente, S. Plerucci, G. Biardi, *Ind. Eng. Chem. Fund.* **1983,** *22* (1), 132-139.
[3] P. J. Clymans, G. F. Froment, *Comp. Chem. Eng.* **1984,** *8* (2), 137-142.
[4] L. P. Hillewaert, J. L. Dierickx, G. F. Froment, *AIChE J.* **1988,** *34* (1), 17-24.
[5] L. J. Broadbelt, S. M. Stark, M. T. Klein, *Comp. Chem. Eng.* **1996,** *20* (2), 113-129.
[6] F. Battin-Leclerc, P. A. Glaude, V. Warth, R. Fournet, G. Scacchi, G. M. Côme, *Chem. Eng. Sci.* **2000,** *55* (15), 2883-2893.
[7] S. Wauters, G. B. Marin, *Chem. Eng. J.* **2001,** *82* (1-3), 267-279.
[8] W. H. Green, P. I. Barton, B. Bhattacharjee, D. M. Matheu, D. A. Schwer, J. Song, R. Sumathi, H. H. Carstensen, A. M. Dean, J. M. Grenda, *Ind. Eng. Chem. Res.* **2001,** *40* (23), 5362-5370.
[9] M. Dente, G. Bozzano, T. Faravelli, A. Marongiu, S. Pierucci, E. Ranzi, *Advanced chemical engineering* **2007,** *32*, 52.
[10] W. H. Green, *Advances in Chemical Engineering* **2007,** *32*, 1-50.
[11] S. Pierucci, E. Ranzi, *Comp. Chem. Eng.* **2008,** *32* (4-5), 805-826.
[12] K. M. Van Geem, M. F. Reyniers, G. B. Marin, J. Song, D. M. Matheu, W. H. Green, *AIChE J.* **2006,** *52* (2), 718-730.

[13] J. Zador, I. G. Zsely, T. Turanyi, M. Ratto, S. Tarantola, A. Saltelli, *J. Phys. Chem. A* **2005,** *109* (43), 9795-9807.

[14] R. G. Susnow, A. M. Dean, W. H. Green, P. Peczak, L. J. Broadbelt, *J. Phys. Chem. A* **1997,** *101* (20), 3731-3740.

[15] M. G. Evans, M. Polanyi, *Proc. Roy. Soc. A* **1936,** *154*, 1333-1360.

[16] M. G. Evans, M. Polanyi, *Trans. Faraday Soc.* **1938,** *1938* (34), 11-29.

[17] P. Blowers, R. Masel, *AIChE J.* **2000,** *46* (10), 2041-2052.

[18] S. W. Benson, J. H. Buss, *J. Chem. Phys.* **1958,** *29* (9), 546-561.

[19] S. W. Benson, *Thermochemical Kinetics;* 1st ed.; John Wiley & Sons Ltd.: New York, **1968**.

[20] P. A. Willems, G. F. Froment, *Ind. Eng. Chem. Res.* **1988,** *27* (11), 1959-1966.

[21] P. A. Willems, G. F. Froment, *Ind. Eng. Chem. Res.* **1988,** *27* (11), 1966-1971.

[22] R. Sumathi, H. H. Carstensen, W. H. Green, *J. Phys. Chem. A* **2001,** *105* (28), 6910-6925.

[23] R. Sumathi, H. H. Carstensen, W. H. Green, *J. Phys. Chem. A* **2001,** *105* (39), 8969-8984.

[24] R. Sumathi, H. H. Carstensen, W. H. Green, *J. Phys. Chem. A* **2002,** *106* (22), 5474-5489.

[25] T. N. Truong, *J. Chem. Phys.* **2000,** *113* (12), 4957-4964.

[26] S. W. Zhang, T. N. Truong, *J. Phys. Chem. A* **2003,** *107* (8), 1138-1147.

[27] M. Saeys, M. F. Reyniers, G. B. Marin, V. Van Speybroeck, M. Waroquier, *AIChE J.* **2004,** *50* (2), 426-444.

[28] M. Saeys, M. F. Reyniers, V. Van Speybroeck, M. Waroquier, G. B. Marin, *ChemPhysChem* **2006,** *7* (1), 188-199.

[29] M. K. Sabbe, M. F. Reyniers, V. Van Speybroeck, M. Waroquier, G. B. Marin, *ChemPhysChem* **2008,** *9* (1), 124-140.

[30] D. L. Baulch, C. J. Cobos, R. A. Cox, C. Esser, P. Frank, T. Just, J. A. Kerr, M. J. Pilling, J. Troe, R. W. Walker, J. Warnatz, *J. Phys. Chem. Ref. Data* **1992,** *21* (3), 411-734.

[31] D. L. Baulch, C. T. Bowman, C. J. Cobos, R. A. Cox, T. Just, J. A. Kerr, M. J. Pilling, D. Stocker, J. Troe, W. Tsang, R. W. Walker, J. Warnatz, *J. Phys. Chem. Ref. Data* **2005,** *34* (3), 757-1397.

[32] W. Tsang, R. F. Hampson, *J. Phys. Chem. Ref. Data* **1986,** *15* (3), 1087-1279.

[33] W. Tsang, *J. Phys. Chem. Ref. Data* **1988,** *17* (2), 887-952.

[34] W. Tsang, *J. Phys. Chem. Ref. Data* **1990,** *19* (1), 1-68.

[35] W. Tsang, *J. Phys. Chem. Ref. Data* **1991,** *20* (2), 221-273.

[36] H. J. Curran, *International Journal of Chemical Kinetics* **2006,** *38* (4), 250-275.

[37] T. Gilbert, T. L. Grebner, I. Fischer, P. Chen, *Journal of Chemical Physics* **1999,** *110* (12), 5485-5488.

[38] Y. Feng, J. T. Niiranen, A. Bencsura, V. D. Knyazev, D. Gutman, W. Tsang, *Journal of Physical Chemistry* **1993,** *97* (4), 871-880.

[39] B. S. Jursic, *Journal of the Chemical Society-Perkin Transactions 2* **1997,** (3), 637-641.

[40] M. T. Nguyen, S. Creve, L. G. Vanquickenborne, *Journal of Physical Chemistry* **1996,** *100* (47), 18422-18425.

[41] H. Fischer, L. Radom, *Angew. Chem. Int. Ed.* **2001,** *40* (8), 1340-1371.

[42] S. S. Shaik, E. Canadell, *Journal of the American Chemical Society* **1990,** *112* (4), 1446-1452.

[43] J. S. Clarke, H. A. Rypkema, J. H. Kroll, N. M. Donahue, J. G. Anderson, *J. Phys. Chem. A* **2000,** *104* (19), 4458-4468.

[44] J. A. Miller, S. J. Klippenstein, *Phys. Chem. Chem. Phys.* **2004,** *6* (6), 1192-1202.

[45] S. J. Klippenstein, J. A. Miller, *J. Phys. Chem. A* **2005,** *109* (19), 4285-4295.

[46] J. Villa, A. Gonzalez-Lafont, J. M. Lluch, D. G. Truhlar, *J. Am. Chem. Soc.* **1998,** *120* (22), 5559-5567.

[47] J. Villa, J. C. Corchado, A. Gonzalez-Lafont, J. M. Lluch, D. G. Truhlar, *J. Am. Chem. Soc.* **1998,** *120* (46), 12141-12142.

[48] J. Villa, J. C. Corchado, A. Gonzalez-Lafont, J. M. Lluch, D. G. Truhlar, *J. Phys. Chem. A* **1999,** *103* (26), 5061-5074.

[49] E. T. Denisov, *Russian Chemical Bulletin* **2004,** *53* (8), 1602-1608.

[50] E. T. Denisov, A. F. Shestakov, N. S. Emel'yanova, *Kinetics and Catalysis* **2006,** *47* (5), 647-661.

[51] E. T. Denisov, *Kinetics and Catalysis* **2008,** *49* (3), 313-324.

[52] J. A. Montgomery, M. J. Frisch, J. W. Ochterski, G. A. Petersson, *J. Chem. Phys.* **1999,** *110* (6), 2822-2827.

[53] Sabbe, M. K.; Vandeputte, A. G. Ab initio group additivity method for the calculation of kinetic parameters for hydrogen abstractions. Unpublished Work, 2008.

[54] M. Saeys, M. F. Reyniers, G. B. Marin, V. Van Speybroeck, M. Waroquier, *J. Phys. Chem. A* **2003,** *107* (43), 9147-9159.

[55] *Gaussian 03, revision B.03,* Gaussian, Inc.: Wallingford CT, 2004

[56] D. K. Malick, G. A. Petersson, J. A. Montgomery, *J. Chem. Phys.* **1998,** *108* (14), 5704-5713.

[57] K. J. Laidler, *Chemical Kinetics;* 3rd ed.; Harper Collins: New York, **1987**.

[58] C. Eckart, *Phys. Rev.* **1930,** *35*, 1303-1309.

[59] T. N. Truong, W. T. Duncan, M. Tirtowidjojo, *Phys. Chem. Chem. Phys.* **1999,** *1* (6), 1061-1065.

[60] N. Kungwan, T. N. Truong, *J. Phys. Chem. A* **2005,** *109* (34), 7742-7750.

[61] A. G. Vandeputte, M. K. Sabbe, M. F. Reyniers, V. Van Speybroeck, M. Waroquier, G. B. Marin, *J. Phys. Chem. A* **2007,** *111* (46), 11771-11786.

[62] M. K. Sabbe, A. G. Vandeputte, M. F. Reyniers, V. Van Speybroeck, M. Waroquier, G. B. Marin, *J. Phys. Chem. A* **2007,** *111* (34), 8416-8428.

[63] E. L. I. Pollak, P. Pechukas, *Journal of the American Chemical Society* **1978,** *100* (10), 2984-2991.

[64] D. R. Coulson, *Journal of the American Chemical Society* **1978,** *100* (10), 2992-2996.

[65] M. A. Baltanas, K. K. Vanraemdonck, G. F. Froment, S. R. Mohedas, *Ind. Eng. Chem. Res.* **1989,** *28* (7), 899-910.

[66] L. K. Huynh, S. Panasewicz, A. Ratkiewicz, T. N. Truong, *J. Phys. Chem. A* **2007,** *111* (11), 2156-2165.

[67] A. Violi, T. N. Truong, A. F. Sarofim, *J. Phys. Chem. A* **2004,** *108* (22), 4846-4852.

[68] D. F. Nava, M. B. Mitchell, L. J. Stief, *Journal of Geophysical Research-Space Physics* **1986,** *91* (A4), 4585-4589.

[69] Chemical Kinetics Database, NIST Standard Reference Database 17, (Web version), Release 1.4.2, Data version 08.09. http://kinetics.*nist. gov/* **2008**.

[70] K. J. Mintz, D. J. Leroy, *Canadian Journal of Chemistry-Revue Canadienne de Chimie* **1978,** *56* (7), 941-949.

[71] L. N. Krasnoperov, J. P. Peng, P. Marshall, *Journal of Physical Chemistry A* **2006,** *110* (9), 3110-3120.

[72] M. K. Sabbe, M. Saeys, M. F. Reyniers, G. B. Marin, V. Van Speybroeck, M. Waroquier, *J. Phys. Chem. A* **2005,** *109* (33), 7466-7480.

[73] M. K. Sabbe, F. De Vleeschouwer, M. F. Reyniers, M. Waroquier, G. B. Marin, *J. Phys. Chem. A* **2008,** *112* (47), 12235-12251.

Received: ((will be filled in by the editorial staff))
Published online: ((will be filled in by the editorial staff))

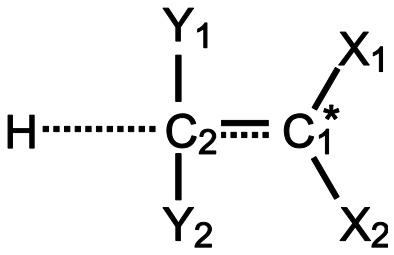

Figure 1: Transition state of a generic hydrogen addition depicting the numbering of the groups.

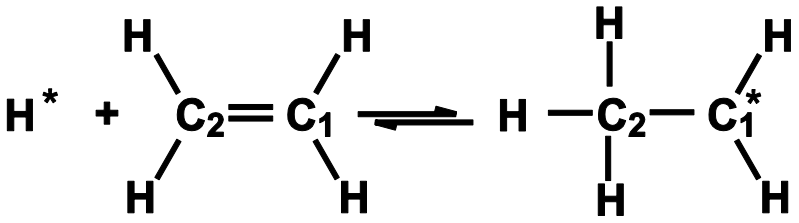

Figure 2: Reference reaction for group additive modeling of hydrogen additions.

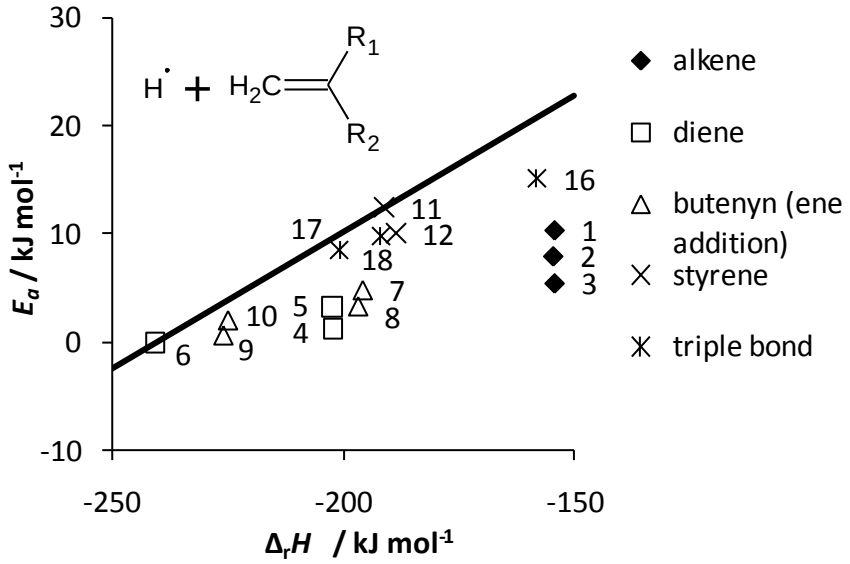

Figure 3: Evans-Polanyi plot for the reactions from Table 3, with indication of the type of unsaturated compound . The full line represents, as upper bond to the dots, the enthalpic contribution to the activation energy: E_a(enth) = 60.7 + 0.25$\Delta_r H°$ (300 K, numbering of Table 3).

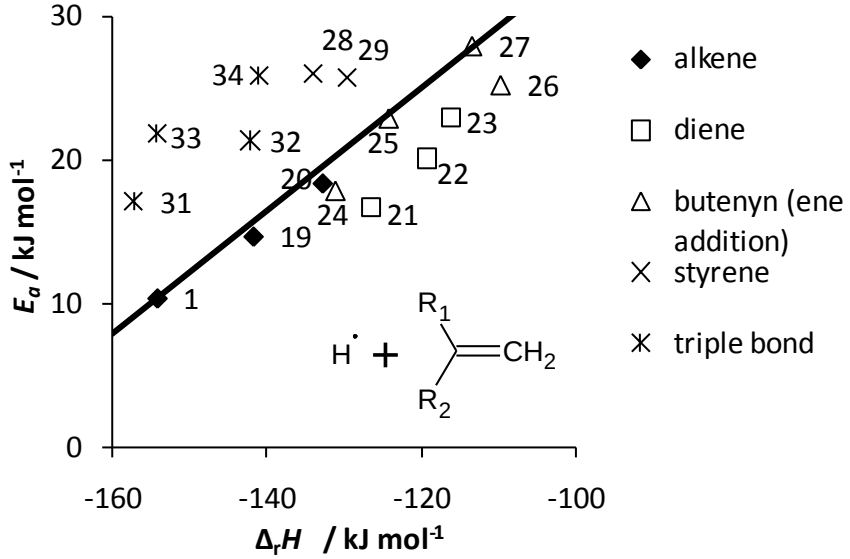

Figure 4: Evans-Polanyi plots for the reactions of Table 4, with indication of the type of unsaturated compound. The full line represents , as upper bond to the dots, the enthalpic contribution to the activation energy, neglecting additions to styrene and triple bonds: E_a(enth)= 76.5 + 0.43$\Delta_r H°$ (300 K, numbering of Table 4).

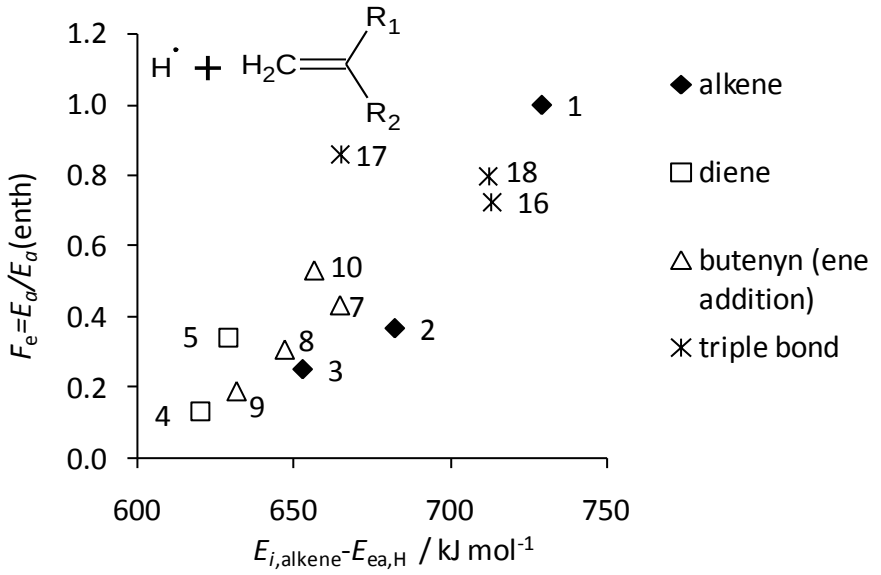

Figure 5: Plot of the electrophilic factor vs. the expected electrophilicity for the reaction of Table 3. The reactions to styrene and to 2-ethenylbuta-1,3-butadiene are excluded since these reactions did not follow the trend (300 K, numbering of Table 3).

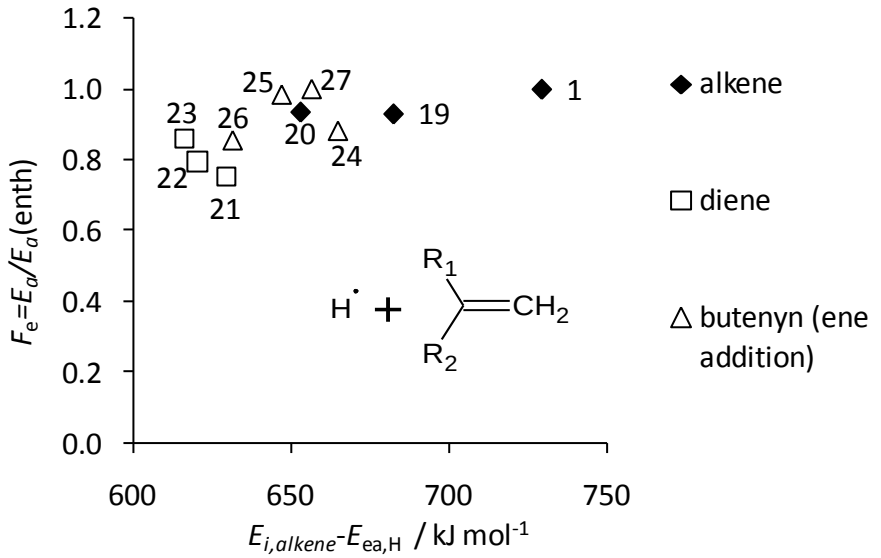

Figure 6: Plot of the electrophilic factor vs. the expected electrophilicity for the reactions of Table 4. The reactions to styrene and to 2-ethenylbuta-1,3-butadiene are excluded since these reactions did not follow the trend (300 K, numbering of Table 4).

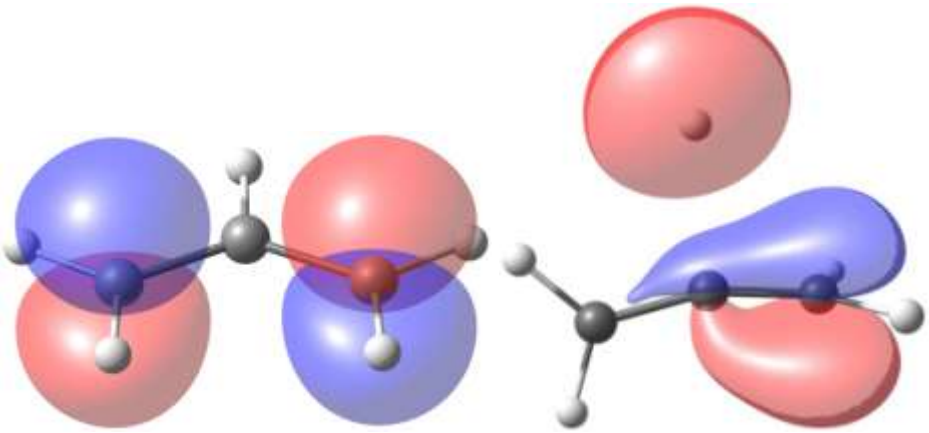

Figure 7: Allyl radical (left) and transition state (right) for the β scission of the allyl radical yielding allene, with HOMO depicted (95% contour).

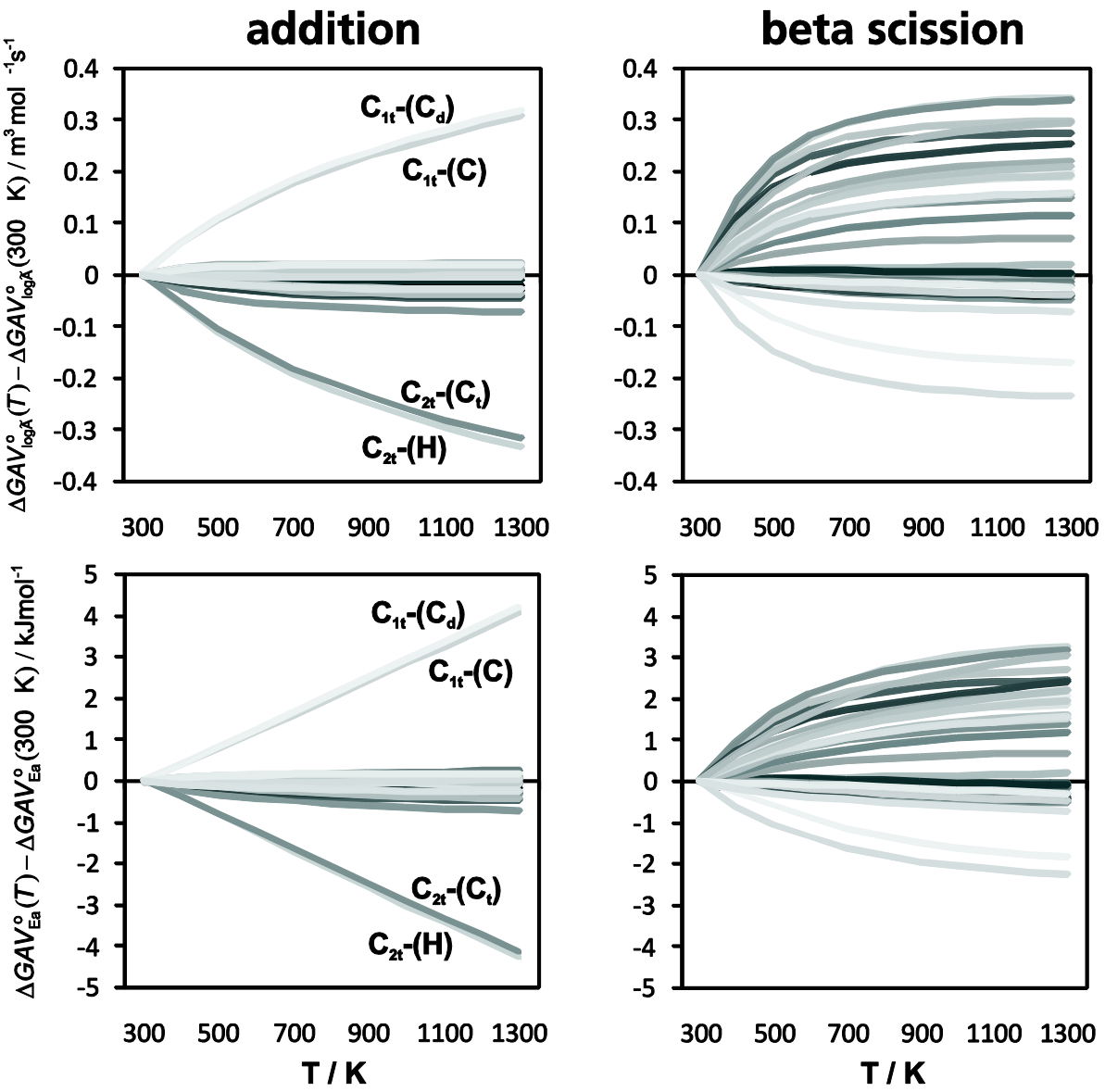

Figure 8: Temperature dependence of the group additive values relative to the Δ*GAV*° at 300 K.

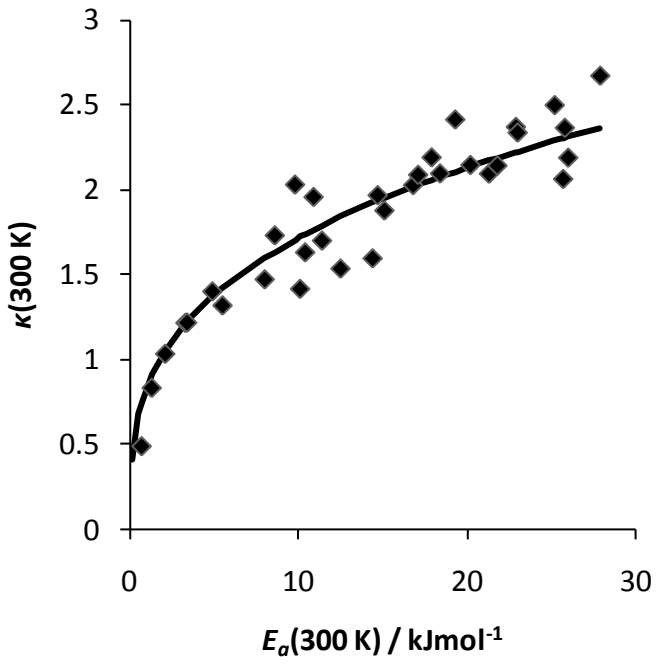

Figure 9: Tunneling coefficients vs. the activation energy at 300 K, for the reactions of Tables 1 and 2 (♦) and the regression of Eq. 10 (full line).

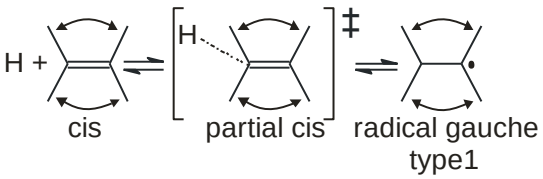

Figure 10: Reactant, transition state and product for the hydrogen addition to 2,3-dimethylbut-2-ene, indicating the non-nearest neighbor interactions neglected by the group additive method.

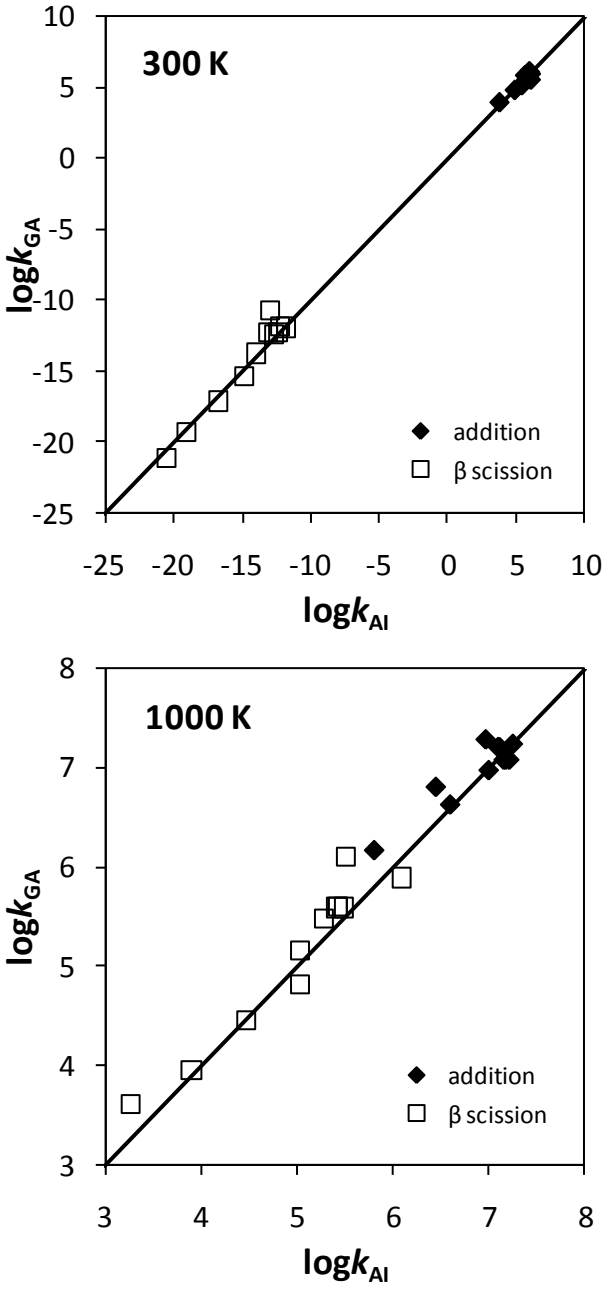

Figure 11: Parity plot of the group additively predicted rate coefficients vs. the ab initio calculated rate coefficients, for the reactions from Table 8 (m^3 mol^{-1} s^{-1}).

Table 1: Comparison of the reaction barrier at 0K ΔE(0 K), the reaction energy at 0 K $\Delta_r E$(0 K), and the high pressure rate coefficient with the respective QCISD(T)/∞ values obtained by Miller and Klippenstein[42,43].

Reaction	ΔE(0 K)		$\Delta_r E$(0 K)		k_{∞} [m^3 mol^{-1} s^{-1}]		
	CBS-QB3	QCISD(T)	CBS-QB3	QCISD(T)	T	CBS-QB3	QCISD(T)
H + 	10.2	11.8[a]	-144.7	-146.4	300 K	$1.0\ 10^6$	$5.9\ 10^5$
					600 K	$7.4\ 10^6$	$5.1\ 10^6$
					1000 K	$2.4\ 10^7$	$1.7\ 10^7$
H + 	16.6	17.9[a]	-146.3	-145.1	300 K	$3.3\ 10^5$	$2.5\ 10^5$
					600 K	$6.8\ 10^6$	$5.8\ 10^6$
					1000 K	$3.1\ 10^7$	$2.7\ 10^7$
H + 	9.3	12.1[b] (10.0)[c]	-182.8	-178.7	300 K	$5.6\ 10^6$	$1.5\ 10^6$
					600 K	$2.7\ 10^7$	$1.4\ 10^7$
					1000 K	$6.9\ 10^7$	$4.2\ 10^7$

[a]Ref. 42 [b]Ref. 43. Value obtained from QCISD(T)/∞ calculation [c]Value obtained after reducing barrier height with 2.1 kJ mol^{-1} in order to bring the rate coefficients in agreement with the experimental measurement of Nava et al. (Ref. 67)

Table 2: Experimental validation: comparison of ab initio calculated rate coefficients (including tunneling) with experimental values based on ρ factors as defined in Eq. 3, averaged out per reaction.

	Reaction	<ρ> addition			<ρ> β scission		
		300K	600K	1000K	300K	600K	1000K
1	H + 	1.4	1.5	1.6	1.4	1.5	1.8
2	H + 	2.7				2.9	1.9
3	H + 	1.4	1.3	1.9	3.1	4.9	2.0
4	H + 	1.5	1.6	2.4	2.2	1.2	1.2
5	H + 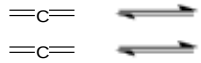	1.1	1.9	2.9	1.2	1.4	2.3
6	H + 	2.4					
7	H +	1.4	1.1	1.3	3.7	1.3	1.4
		<ρ>	**1.7**	**1.5**	**2.0**	**2.3**	**2.2**	**1.8**
		$<\rho>_{mean}$	**1.9**					

Table 3: Tunneling coefficients, pre-exponential factors, activations energies, rate coefficients (including tunneling contributions) and reaction enthalpies for hydrogen additions and β scissions, evaluating the influence of substituents at the C_1 carbon atom. The Arrhenius parameters have been determined as described in section 2.2 (E_a and $\Delta_r H°$ in kJ mol^{-1}, 300 K).

				κ	addition [m³ mol^{-1} s^{-1}]			β scission [s^{-1}]			$\Delta_r H°$
					log$A$	E_a	k_κ	log$A$	E_a	k_κ	
1	H	+		1.63	7.612	10.4	$1.0\ 10^{6}$	12.790	156.3	$6.1\ 10^{-15}$	-145.9
2	H	+		1.48	7.328	8.0	$1.3\ 10^{6}$	13.245	154.2	$3.7\ 10^{-14}$	-146.2
3	H	+		1.32	7.379	5.5	$3.5\ 10^{6}$	13.234	151.4	$9.8\ 10^{-14}$	-145.9
4	H	+		1.22	7.577	3.3	$1.2\ 10^{7}$	13.507	197.2	$1.8\ 10^{-21}$	-193.9
5	H	+		0.83	7.313	1.3	$1.0\ 10^{7}$	12.942	195.1	$7.8\ 10^{-22}$	-193.8
6	H	+		-	6.967	0	$9.3\ 10^{6}$	12.852	231.2	$3.9\ 10^{-28}$	-232.4
7	H	+		1.40	7.275	4.9	$3.7\ 10^{6}$	13.101	192.3	$5.8\ 10^{-21}$	-187.4
8	H	+		1.22	7.324	3.4	$6.6\ 10^{6}$	13.187	191.8	$7.5\ 10^{-21}$	-188.4
9	H	+		0.49	7.278	0.7	$7.0\ 10^{6}$	13.263	218.4	$8.4\ 10^{-26}$	-217.7
10	H	+		1.04	7.261	2.1	$8.1\ 10^{6}$	12.283	218.8	$1.6\ 10^{-26}$	-216.7
11	H	+		1.54	6.718	12.5	$5.4\ 10^{4}$	13.282	195.3	$2.9\ 10^{-21}$	-182.8
12	H	+		1.42	7.169	10.1	$3.7\ 10^{5}$	12.735	190.4	$5.4\ 10^{-21}$	-180.3
13	H	+		1.70	7.600	11.4	$7.0\ 10^{5}$	13.200	164.3	$6.7\ 10^{-16}$	-152.9
14	H	+		1.60	7.415	14.4	$1.3\ 10^{5}$	14.043	257.9	$2.2\ 10^{-31}$	-243.5
15	H	+		1.96	7.224	10.9	$4.2\ 10^{5}$	13.109	255.8	$7.3\ 10^{-32}$	-244.9
16	H	+		1.88	7.802	15.1	$2.8\ 10^{5}$	13.638	164.9	$1.6\ 10^{-15}$	-149.8
17	H	+		1.74	7.368	8.6	$1.3\ 10^{6}$	13.789	201.2	$9.9\ 10^{-22}$	-192.6
18	H	+		2.04	8.144	9.8	$5.6\ 10^{6}$	13.091	193.5	$5.1\ 10^{-21}$	-183.7

Table 4: Tunneling coefficients, pre-exponential factors, activations energies, rate coefficients (including tunneling contributions) and reaction enthalpies for hydrogen additions and β scissions, evaluating the influence of substituents at the C_2 carbon atom The Arrhenius parameters have been determined as described in section 2.2 (E_a and $\Delta_r H°$ in kJ mol^{-1}, 300 K).

			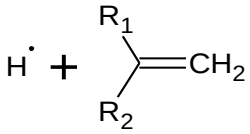	κ	addition [m^3 mol^{-1} s^{-1}]			β scission [s^{-1}]			$\Delta_r H°$
					log$A$	E_a	k	log$A$	E_a	k	
19	H	+		1.97	7.123	14.7	7.2 10^4	13.095	148.1	4.0 10^{-13}	-133.4
20	H	+		2.10	6.885	18.4	1.0 10^4	12.725	142.8	1.5 10^{-12}	-124.4
21	H	+		2.03	7.479	16.8	7.3 10^4	12.916	135.0	5.2 10^{-11}	-118.2
22	H	+		2.15	7.005	20.2	6.6 10^3	12.513	131.2	1.0 10^{-10}	-111.0
23	H	+		2.34	6.814	23.0	1.5 10^3	12.345	130.9	8.4 10^{-11}	-107.9
24	H	+		2.20	7.153	17.9	2.4 10^4	12.684	140.7	3.4 10^{-12}	-122.8
25	H	+		2.38	6.970	22.9	2.3 10^3	12.575	138.8	6.1 10^{-12}	-115.9
26	H	+		2.50	7.105	25.2	1.3 10^3	12.601	126.6	9.0 10^{-10}	-101.4
27	H	+		2.68	7.086	27.9	4.5 10^2	12.504	133.0	5.9 10^{-11}	-105.1
28	H	+		2.19	6.658	26.0	3.0 10^2	12.609	151.6	3.6 10^{-14}	-125.6
29	H	+		2.07	6.827	25.7	4.7 10^2	12.578	147.0	2.0 10^{-13}	-121.3
30	H	+		2.42	7.666	19.3	4.9 10^4	14.008	257.2	4.1 10^{-31}	-237.9
31	H	+		2.09	8.179	17.1	3.3 10^5	13.556	166.0	9.4 10^{-16}	-148.9
32	H	+		2.10	7.545	21.3	1.4 10^4	13.496	155.3	6.0 10^{-14}	-134.0
33	H	+		2.15	7.412	21.8	8.9 10^3	14.035	167.7	1.5 10^{-15}	-145.9
34	H	+		2.37	8.094	25.8	9.5 10^3	13.382	158.7	1.3 10^{-14}	-132.9

Table 5: Group additive values for hydrogen addition (m^3 mol^{-1} s^{-1} and kJ mol^{-1}).

Nr.	group	300 K				1000 K			
		addition		β scission		addition		β scission	
		log$\tilde{A}$	E_a	log$\tilde{A}$	E_a	log$\tilde{A}$	E_a	log$\tilde{A}$	E_a
Reference reaction		7.010	10.4	12.012	156.3	7.726	18.5	12.580	162.4
C_1-1	C_1-(C)(H)	+0.017	-2.4	+0.154	-2.1	+0.019	−2.4	+0.224	−1.4
C_1-2	C_1-$(C)_2$	+0.068	-4.9	+0.268	-4.9	+0.072	−4.9	+0.452	−3.2
C_1-3	C_1-(C_d)(H)	-0.035	-7.1	+0.717	+40.9	−0.024	−7.0	+0.861	+42.2
C_1-4	C_1-(C_d)(C)	+0.002	-9.1	+0.152	+38.8	+0.023	−8.9	+0.303	+40.2
C_1-5	C_1-$(C_d)_2$	-0.043	-10.4	+0.062	+74.9	−0.022	−11.4	+0.273	+76.9
C_1-6	C_1-(C_t)(H)	-0.036	-5.5	+0.311	+36.0	−0.028	−5.4	+0.420	+37.0
C_1-7	C_1-(C_t)(C)	+0.013	-7.0	+0.096	+35.5	+0.022	−6.9	+0.244	+36.9
C_1-8	C_1-$(C_t)(C_d)$	-0.033	-9.7	+0.473	+62.1	−0.012	−9.5	+0.663	+63.9
C_1-9	C_1-$(C_t)_2$	-0.050	-8.3	-0.507	+62.5	−0.037	−8.2	−0.308	+64.5
C_1-10	C_1-(C_b)(H)	-0.593	+2.1	+0.492	+39.0	−0.595	+2.1	+0.642	+40.4
C_1-11	C_1-(C_b)(C)	-0.142	-0.3	-0.055	+34.1	−0.133	−0.3	+0.128	+35.9
C_1-12	$C_{1,allene}$-	-0.012	+1.0	+0.711	+8.0	−0.048	+0.6	+0.989	+10.7
C_1-13	$C_{1,alleneII}$-(C)(H)	+0.050	-4.9	+0.035	+0.7	+0.071	−4.7	+0.018	+0.6
C_1-14	$C_{1,alleneII}$-$(C)_2$	-0.141	-8.4	-0.598	-1.4	−0.165	−8.7	−0.662	−2.0
C_1-15	C_{1t}-(C)	-0.553	-2.0	+0.082	-1.1	−0.299	+0.8	+0.048	−1.5
C_1-16	C_{1t}-(C_d)	-0.811	-8.5	-0.068	+35.2	−0.547	−5.5	−0.225	+33.6
C_1-17	C_{1t}-(C_t)	-0.035	-7.3	-0.465	+27.5	−0.036	−7.3	−0.990	+25.4
C_2-1	C_2-(C)(H)	-0.188	+4.3	+0.481	-8.2	−0.217	+4.0	+0.475	−8.3
C_2-2	C_2-$(C)_2$	-0.426	+8.0	+0.412	-13.5	−0.493	+7.4	+0.370	−13.9
C_2-3	C_2-(C_d)(H)	-0.133	+6.4	+0.302	-21.3	−0.132	+6.4	+0.305	−21.3
C_2-4	C_2-(C_d)(C)	-0.306	+9.8	+0.200	-25.1	−0.323	+9.7	+0.164	−25.5
C_2-5	C_2-$(C_d)_2$	-0.196	+12.6	+0.032	-25.4	−0.196	+12.7	−0.005	−25.8
C_2-6	C_2-(C_t)(H)	-0.158	+7.5	+0.070	-15.6	−0.161	+7.6	+0.086	−15.4
C_2-7	C_2-(C_t)(C)	-0.341	+12.5	+0.262	-17.5	−0.366	+12.4	+0.226	−17.9
C_2-8	C_2-$(C_t)(C_d)$	-0.206	+14.8	+0.288	-29.7	−0.182	+15.1	+0.282	−29.7
C_2-9	C_2-$(C_t)_2$	-0.225	+17.5	+0.492	-23.3	−0.204	+17.8	+0.481	−23.4
C_2-10	C_2-(C_b)(H)	-0.653	+15.6	-0.306	-4.7	−0.663	+15.5	−0.300	−4.7
C_2-11	C_2-(C_b)(C)	-0.484	+15.3	-0.036	-9.3	−0.517	+15.1	−0.052	−9.5
C_2-12	$C_{2,allene}$	+0.054	+8.9	+1.695	+100.9	+0.014	+8.6	+1.938	+103.0
C_2-13	C_{2t}-(H)	+0.868	+6.7	+1.544	+9.7	+0.595	+3.7	+1.879	+12.8
C_2-14	C_{2t}-(C)	+0.058	+10.9	+1.484	-1.0	+0.015	+10.5	+1.755	+1.3
C_2-15	C_{2t}-(C_d)	+0.101	+11.4	+1.722	+11.4	+0.077	+11.2	+2.016	+14.0
C_2-16	C_{2t}-(C_t)	+0.783	+15.4	+1.370	+2.4	+0.523	+12.5	+1.700	+5.3

Table 6: Single-event Arrhenius parameters for the reference reaction H+ethene.

T	addition		β scission	
	$\log\tilde{A}_{ref}$	$E_{a,ref}$	$\log\tilde{A}_{ref}$	$E_{a,ref}$
K	$m^3\ mol^{-1}\ s^{-1}$	kJ mol^{-1}	s^{-1}	kJ mol^{-1}
300	7.010	10.4	12.012	156.3
400	7.153	11.3	12.150	157.2
500	7.283	12.4	12.265	158.1
600	7.396	13.6	12.358	159.1
700	7.494	14.8	12.433	160.0
800	7.580	16.0	12.493	160.9
900	7.657	17.3	12.541	161.7
1000	7.726	18.5	12.580	162.4
1100	7.788	19.8	12.611	163.0
1200	7.845	21.0	12.637	163.6
1300	7.897	22.3	12.659	164.1

Table 7: Group additive model validation: comparison of group additive prediction with ab initio calculation for the tunneling coefficients, pre-exponential factors and activation energies of additions (a) and β scission (β) (1000 K tunneling contributions are neglected).

	Reaction		300 K			1000 K	
		κ/κ_{AI}	$\frac{A_{GA}}{A_{AI}}$	$E_{a,GA}$ -$E_{a,AI}$	$\frac{A_{GA}}{A_{AI}}$	$E_{a,GA}$ -$E_{a,AI}$
1a	H +   	1.01	0.92	+1.1	0.94	+1.2
1 β			1.24	-0.5	1.18	-0.6
2a	H +   	1.01	0.95	+1.0	0.97	+1.1
2 β			0.78	-5.7	0.76	-5.8
3a	H +   	1.01	1.21	+0.8	1.20	+0.7
3 β			1.35	-0.9	1.36	-0.8
4a	H +   	1.05	1.25	-0.3	1.27	-0.2
4 β			1.27	-0.7	1.29	-0.6
5a	H +   	1.12	4.32	+5.3	4.44	+5.4
5 β			0.93	-12.5	0.88	-12.6
6a	H +   	1.14	1.15	+3.7	1.16	+3.6
6 β			0.66	-0.1	0.63	-0.3
7a	H +   	0.93	2.84	+1.3	2.72	+1.1
7 β			1.36	-1.4	1.44	-1.1
8a	H + 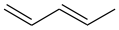  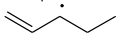	0.91	1.01	+0.6	1.05	+0.7
8 β			1.37	+1.3	1.32	+1.1
9a	H + 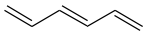  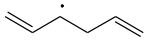	0.90	0.89	-0.7	0.91	-0.7
9 β			1.35	+2.4	1.31	+2.3
10a	H +   	1.08	2.42	+1.2	2.43	+1.2
10 β			0.90	+3.1	0.90	+3.1
11a	H +   	0.86	1.22	-0.1	1.26	+0.1
11 β			4.72	+6.5	5.22	+6.8

Table 8:Group additive validation: comparison of group additive prediction with ab initio calculation for the rate coefficients of additions (a) and β scission (β), and equilibrium coefficients (1000 K tunneling contributions are neglected).

	Reaction	300 K			1000 K		
		k_{AI}	$\frac{k_{GA,\kappa}}{k_{AI}}$	$\frac{K_{GA}^{eq}}{K_{AI}^{eq}}$	k_{AI}	$\frac{k_{GA,\kappa}}{k_{AI}}$	$\frac{K_{GA}^{eq}}{K_{AI}^{eq}}$
1a	H +   	$5.8\ 10^{5}$	0.63	0.38	$1.5\ 10^{7}$	0.82	0.64
1 β		$3.7\ 10^{-13}$	1.66		$3.1\ 10^{5}$	1.28	
2a	H +   	$5.3\ 10^{5}$	0.68	0.08	$1.4\ 10^{7}$	0.86	0.57
2 β		$7.2\ 10^{-14}$	8.53		$2.6\ 10^{5}$	1.52	
3a	H +   	$7.6\ 10^{4}$	0.93	0.46	$3.9\ 10^{6}$	1.11	0.73
3 β		$2.0\ 10^{-13}$	2.02		$2.7\ 10^{5}$	1.51	
4a	H +   	$9.0\ 10^{5}$	1.53	0.82	$1.2\ 10^{7}$	1.31	0.94
4 β		$1.1\ 10^{-14}$	1.87		$1.1\ 10^{5}$	1.39	
5a	H +   	$2.6\ 10^{5}$	0.59	0.004	$2.8\ 10^{6}$	2.33	0.58
5 β		$1.1\ 10^{-13}$	162.98		$3.2\ 10^{5}$	4.02	
6a	H +   	$1.2\ 10^{6}$	0.31	0.37	$1.6\ 10^{7}$	0.75	1.16
6 β		$1.5\ 10^{-12}$	0.83		$1.2\ 10^{6}$	0.65	
7a	H +   	$5.8\ 10^{3}$	1.73	0.71	$6.4\ 10^{5}$	2.39	1.45
7 β		$6.2\ 10^{-13}$	2.43		$1.9\ 10^{5}$	1.65	
8a	H + 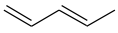  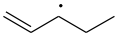	$1.2\ 10^{6}$	0.77	0.95	$9.8\ 10^{6}$	0.97	0.84
8 β		$7.8\ 10^{-20}$	0.81		$7.9\ 10^{3}$	1.16	
9a	H + 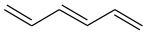  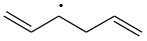	$8.5\ 10^{5}$	1.14	2.27	$1.7\ 10^{7}$	0.99	1.00
9 β		$1.7\ 10^{-17}$	0.50		$3.0\ 10^{4}$	1.00	
10a	H +   	$4.4\ 10^{5}$	1.70	5.42	$9.1\ 10^{6}$	2.10	3.38
10 β		$1.5\ 10^{-15}$	0.31		$1.1\ 10^{5}$	0.62	
11a	H +   	$1.0\ 10^{6}$	1.18	3.55	$1.3\ 10^{7}$	1.25	0.54
11 β		$2.8\ 10^{-21}$	0.33		$1.8\ 10^{3}$	2.30	
ρ addition			1.6			1.5	
ρ β scission			17.3			1.7	
ρ β scission (reaction 5 excluded)			2.7			1.5	

Table 9: Group additive model validation: comparison of group additive prediction (including tunneling correction) with experimental values based on ρ factors as defined in Eq. 3, averaged out per reaction.

	Reaction	<ρ> addition			<ρ> β scission		
		300K	600K	1000K	300K	600K	1000K
1	H +   	1.7			1.3	1.3	
2	H +   	1.5			1.3	2.3	1.8
3	H +   	1.3	1.4	2.0	1.1	1.8	1.8
4	H +   	1.7			8.2	1.3	1.1
5	H +  	4.9					
6	H +   	5.5					
7	H +   	1.5					
		<ρ>	2.6	1.4	2.0	3.0	1.7	1.6
		$<\rho>_{mean}$	2.0					